Synthesis, Characterization and Properties Evaluation of Polybutadiene Rubber Based Nanocomposites: *Ex situ* and *In situ* Approaches

By

Bhavin H. Patel

12MCHC17

DEPARTMENT OF CHEMICAL ENGINEERING

AHMEDABAD-382481

May 2014

Synthesis, Characterization and Properties Evaluation of Polybutadiene Rubber Based Nanocomposites: *Ex situ* and *In situ* Approaches

Major Project Report

Submitted in partial fulfillment of the requirements

For the Degree of

Master of Technology in Chemical Engineering

(Chemical Process And Plant Design)

By

Bhavin H. Patel

(12MCHC17)

Guided By

Dr. M. Maiti

Dr. S. S. Patel

DEPARTMENT OF CHEMICAL ENGINEERING

AHMEDABAD-382481

May 2014

Declaration

This is to certify that

1. The thesis comprises my original work towards the degree of Master of Technology in Chemical Engineering (Chemical Process And Plant Design) at Institute of Technology, Nirma University and has not been submitted elsewhere for a degree.
2. Due acknowledgment has been made in the text to all other material used.

Bhavin H. Patel

12MCHC17

Undertaking for Originality of the Work

I Bhavin Patel, 12MCHC17, give undertaking that the major project entitled "**Synthesis, Characterization and Properties Evaluation of Polybutadiene Rubber Based Nanocomposites:*ex situ* and *in situ* approaches**" submitted by me, towards the partial fulfillment of the requirements for the degree of Master of Technology in Chemical Engineering (Chemical process and plant design) of Nirma University, Ahmedabad is the original work carried out by me and I give assurance that no attempt of plagiarism had been made. Due acknowledgement has been made in the text to all other material used.

I understand, that in the event of any similarity found subsequently with any published work or dissertation work elsewhere, it will result in severe disciplinary action.

Bhavin Patel

Date:

Place:

Endorsed by:

(Signature of Guide)

Certificate

This is to certify that the Major Project Report entitled "**Synthesis, Characterization and Properties Evaluation of Polybutadiene Rubber Based Nanocomposites:*ex situ* and *in situ* approaches**" submitted by **Bhavin H. Patel (12MCHC17)**, Towards the partial fulfillment of the requirements for the award of Degree of Master of Technology in Chemical Engineering (Chemical Process And Plant Design) of Institute of Technology, Nirma University, Ahmadabad is the record of work carried out by him under our supervision and guidance. In our opinion, the submitted work has reached a level required for being accepted for examination.The result embodied in this major project, to the best of our knowledge, has not been submitted to any other University or Institution for award of any degree.

Dr. M. Maiti
Senior Manager, RTG-VMD
Reliance Industries Limited
Vadodara,
Gujarat.

Dr S. S. Patel
Professor and Head
Department of Chemical Engineering,
Institute of Technology,
Nirma University,
Ahmedabad.

Dr K. Kotecha
Director,
Institute of Technology,
Nirma University,
Ahmedabad.

Acknowledgments

Before we embark upon the details of my project work, let me take this opportunity to express my heartiest gratitude towards the people who have provided invaluable help and support. Words will always be inadequate to express my proud respect and a deep sense of indebtedness to my guide **Dr. M. Maiti** (Senior Manager, RTG-VMD, Reliance Industries Ltd., Vadodara) for their guidance and motivation throughout. They have devoted significant amount of their valuable time to plan and discuss the thesis work as well as all the experiments that I have carried out during my dissertation work. It was great privilege and honour to have a guide like them who would constantly stand beside me whenever I was performing experiments or had doubts. My sincere thanks and due respect to **Dr. S. S. Patel,** (HOD, Chemical Engineering Department, IT, NU) for his constant cooperation, valuable suggestions and guidance throughout this dissertation work.

I would like to thank Dr. R.V. Jasra (Head, RTG-VMD) for giving me this opportunity to work on this project.

I would like to thank Dr. K. Kotecha (Director, Nirma Institute of Technology) and I express my deep sense of gratitude to Dr. R. Mewada (Associate Prof. and Head, M.Tech., Chemical process and plant design, Chemical Engineering Department, Nirma Institute of *Technology*) for his suggestions and esteemed guidance throughout this research.

I express my deep sense of gratitude to Dr. G. Basak (Manager, RTG-VMD) for his valuable suggestions and guidance throught my dissertation work.

I am thankful to Dr. V. Srivastava for being an intellectual support and Chirag sir for adding to my laboratory skills throughout my dissertation work, elastomer group, RIL, Vadodara. I am also thankful to Mr. Kalpash Bhatt of PBR-II lab, Mr. N.F. Patel of polymer group, Mr. Haribhai Mackwana, Ms. Anagha Purohit and Ms. Rashmi Dave of analytical department. I express my especially thanks to colleagues Ketul, Sudeep, Shakti, Rima and Rushi at RIL for their unconditional help and encouragement.

Last, but not the least, no words are enough to acknowledge constant support of my family members and friends because of whom I am able to complete the major project work successfully.

Bhavin H. Patel

Abstract

In the present study, elastomer nanocomposites based on polybutadiene rubber and different kind of nanofillers were prepared either by using *in situ* or *ex situ* methods. The effects of different nanofiller and their compounding on the physico-mechanical and thermal properties of BR nanocomposites were investigated. Nanofillers like nanosilica, sepiolite, pangel, hydrotalcite, montmorillonite, and CNT were used as reinforcing agent. The textural properties of the nanomaterials were characterized by powder X-ray diffraction (XRD), and BET-surface area measurements. The mechanical properties of various nanocomposites prepared by *ex situ* method were compared with composites made of conventional fillers such as carbon black and silica. The result indicates that composites prepared from nanofillers show higher mechanical properties as compared to conventionally filled composites. It is also observed that the performance of nanosilica in BR matrix enhanced in presence of silane as a coupling agent. The composite containing 3 phr loaded Cloisite 20A showed 245% improvement in tensile strength compared to the matrix devoid of nanomaterial. Also the composite containing 5 phr loaded CNT showed 137% improvement in tensile strength. Thermal analysis of the nanocomposites and gum BR vulcanizates itself was done by thermogravimetric analyzer. It showed that the addition of nanofiller increses the thermal stability of the nanocomposites. This may be due to the heat shielding effect of the incorporated nanofillers in the polymer matrix.

The effect of best nanofillers, obtained from *ex situ* method such as CNT and nanosilica-silane at minimum filler concentration, on the mechanical properties of BR nanocomposites is further studied via *in situ* process. A maximum of 72 % improvement in tensile strength is accomplished using 1 phr nanosilica loaded BR nanocomposites as compared to gum BR vulcanizate. The swelling and thermo gravimetric analysis results of all the BR based nanocomposites are in good agreement with mechanical properties of the same.

Keywords : polybutadiene rubber; nanocomposites; *in situ* and *ex situ* processes; mechanical properties; thermal properties

Contents

List of Figures

List of Tables

Nomenclatures

M_L	Minimum torque (lb.in)
M_H	Maximum torque (lb.in)
t_{s2}	Scorch time
t_{90}	time to 90% cure
n	Integer for 1^{st} order diffraction
λ	Wavelength of incident x-ray beam (Å)
d	Distance between atomic layer in crystal (nm)
θ	Angle of incidence
ν	Cross link density (ρ/Mc)
ρ	Rubber density (g/cm^3)
Mc	molecular weight of rubber
Vs	Molar volume of solvent
Vr	Volume fraction of swollen gel
x	interaction constant
θr	Angle of rebound
θf	Angle of fall
P	Pressure (Kg/cm^2)
MPa	Mega pascal
η	Intrinsic viscosity (dL/g)
Mv	Viscosity average molecular weight
Mt	Mass up taken (g)
T_{max}	Temperature corresponding to the maximum value in the derivative thermogram
T_{onset}	Temperature corresponding to 5% degradation
BR	Polybutadiene rubber
6PPD	(1,3-Dimethylbutyl)-N'-phenyl-p-phenylenediamine
CBS	N-Cyclohexyl-2-benzothiazole-sulfenamide
DTBPC	Di-tert-butyl-para-cresol
Phr	Per hundred gram of rubber
NCs	Polymer nanocomposites
MWCNT	Multi walled carbon nanotubes
POSS	Polyhedral oligomeric silsequioxane
DEAC	Diethylaluminium Chloride
TEAL	Triethylaluminium
XRD	X-ray diffraction
TGA	Thermogravimetric analysis
DTG	Derivative thermogravimetric analysis

Chapter 1

Introduction

1.1 Introduction to rubber technology

Early in the nineteenth century, the products of rubber were subjects of great curiosity which was flexible, elastic, tough, waterproof, and quite impermeable to water and air but of no real study. The men who tried it for a wide variety of uses are Macintosh and Hancock in Great Britain and Charles Goodyear in the US. But there were two major troubles. The rubber got stiff and hard in cold weather and soft and sticky in hot weather. In 1839 Charles Goodyear discovered that when rubber is heated with sulphur it becomes drastically changed. The strength and elasticity are greatly increased. It does not get hardened in cold weather and soft in hot weather any more. These men also discovered methods for kneading the tough, crude rubber so that it becomes soft enough for the incorporation of sulphur and other powders. These developments were the foundation of the rubber industries.

The stories of these two men, Goodyear's "Gum Elastic" and Hancock's "Personal Narrative" cover the methods they developed for processing. Compounding and vulcanizing rubber and the application of those methods in the manufacturing of rubber goods. On the basis of their work, a small but flourishing rubber industry grew up in the US and Europe. Its products were raincoats, foot wear, solid tires for carriages, hose and miscellaneous items. However, by 1890 Bouchardat, Tilden, and Wallach had all made synthetic rubber-like products from the polymerization of isoprene. The pneumatic tire was patented by Dunlop in England in 1888.

Over the past 20 decades, the importance of rubber to civilized living has increased at a constant accelerated pace. This is due to its certain mechanical and physical properties. First and foremost is elasticity. Allied to elasticity is flexibility, a thin sheet of rubber is almost as flexible as a handkerchief. The rubber is also elastic; however, the handkerchief is not. Of almost equal importance with elasticity are strength and toughness. The high strength and great toughness of rubber permit the use of its elastic qualities under conditions in which most other elastic materials would fail. Along with these properties, rubber should possess excellent resistance to cutting, tearing and toughness. Hence, it has a relatively long, useful life under a wide variety of condition.

A very important and almost unique quality of uncured rubber is "building tack" when two fresh surfaces of milled rubber are pressed together, they coalesce to form a single piece. Another quality of great importance is the ease with which properties such as hardness, strength and abrasion resistance can be modified by compounding techniques. This has an additional advantage that forms rubber more inert to the deteriorating effects of the atmosphere and of many chemicals. Hence, it has a relatively long, useful life under a wide variety of condition.

1.2 Composites

A composite is defined as a heterogeneous mixture of two or more materials which does not lose the characteristics of each component. This combination of materials brings about new desirable properties[1]. A composite consists of a continuous phase, termed as the matrix, and a dispersed phase termed as reinforce or filler. The filler may be reinforcing or non-reinforcing type. In case of reinforcing filler, the filler improves the properties of the matrix material. The filler may be organic or inorganic; particulate or fibrous. For particulate type of reinforcer, the reinforcing effect depends on the particle size, shape; size distribution etc. for fibrous type of reinforcer, the reinforcing effect mainly depends on the l/d ratio and the orientation of the fibres [2]. Naturally occurring composites include bone, bamboo, rock, and many other biological and geological materials. Polymer matrices along with naturally occurring mineral fillers such as silica, clay, mica and calcium carbonate or synthetic fillers like carbon black, glass fibers, carbon fibers etc. from polymer composites [3].

1.2.1 Advantages of composite materials

Composites have many engineering advantages over synthetic polymers and copolymers. Some of these advantages are:

Reinforcement of the resin resulting in increased tensile strength, flexural strength, compression strength, impact strength, rigidity and combination of these properties.

- Increased dimensional stability.
- Improved fire retardancy.
- Corrosion protection.
- Improved electrical properties; reduction of dielectric constant.
- Improved processibility; controlled viscosities, good mixing, controlled orientation of fibers.

1.3 Nanocomposites

A nanocomposite is defined as the composite of two materials, one having the dimension of nanometric level at least in one dimension. In polymer nanocomposites (PNC), the fillers are dispersed on a nanolevel[4]. Three types of nanocomposites can be distinguished depending upon the number of dimensions of the dispersed particles in the nanometer range as follows:

- Iso dimensional nanofiller result when the three dimensions are in the order of nanometers such as spherical silica nanoparticles obtained by in situ sol gel methods.
- When two dimensions are in nanometer scale while the third is larger, an elongated structure results as e.g: Carbon nanotubes which are extensively studied as reinforcing nanofiller.
- The third type of nanocomposite is characterized by only one dimension of the filler in the nanometer range. Here the filler is in the form of sheets of one to a few nanometer thickness. Clays and layered silicates belong to this family and the composites are known as polymer clay nanocomposites. In polymer nanocomposites the fillers are dispersed in nano level.

1.3.1 Classification of nanocomposites

Depending on the nature of filler, type of dispersion, and method of preparation, the nanocomposites can be divided into subclasses. With the variation in nanofillers, mainly the following types of nanocomposites can be obtained [5]:

1. Clay-based nanocomposites
2. Silica-based nanocomposites
3. Polyhedral oligomeric silsequioxane (POSS)-based nanocomposites
4. Carbon nanotubes-based nanocomposites
5. Nanocomposites based on other nanofillers like metal oxides, hydroxides, and carbonates.

1.3.2 Nanocomposite structure

In general, the structures of polymer nanocomposites are classified according to the level of intercalation and exfoliation of polymer chains into the filler galleries. Various parameters including nature of nanofiller, organic modifier, polymer matrix and preparation method are affective on the intercalation and exfoliation level. Therefore depending on the nature and properties of filler and polymer as well as preparation methodology of nanocomposite, different composite micro-structures can be obtained [5].

Phase separated structure

When the organic polymer is interacted with inorganic filler, the polymer is unable to intercalate within the filler layers and it is dispersed as aggregates or particles with layers stacked together within the polymer matrix. The obtained composite structure is considered as "phase separated". The properties of phase separated polymer/filler composites are in the range of traditional micro composites.

Intercalated structure

When one or more polymer chains are inserted into the inner layer space of the nanofiller and increase the inter layer spacing, but the periodic array of the filler layer still exists, the intercalated nanocomposite is formed. The presence of polymer chains in the galleries decreases of electrostatic forces between the layers but it is not totally dissolved. A well-ordered multilayer hybrid morphology with a high interference interactions consisted of polymer chains and nanofiller layer is obtained in this configuration.

Exfoliated structure

Exfoliated structure is obtained when the insertion of polymer chains into the filler galleries causes to the separation of the layers from one another and individual layers are dispersed within the polymer matrix. At all, when the polymer chains increases the interlayer spacing more than 80-100 Å, the exfoliated structure is obtained. Due to the well dispersion of individual nanofiller layers, high aspect ratio is obtained and lower filler content is needed for exfoliated nanocomposites. Also most significant improvement in polymer properties is obtained due to the large surface interactions between polymer and filler. Various polymer/clay structural configurations are shown in Figure 1.1 [5].

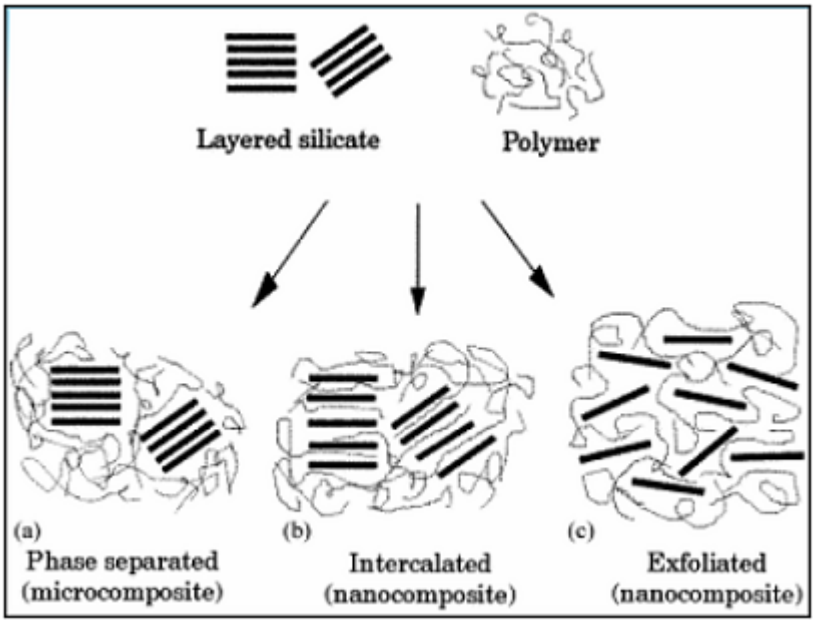

Figure 1.1: Various structures of polymer/layered silicate nanocomposites

1.3.3 Preparation of polymer nanocomposites

Many efforts have been made for the preparation of intercalated and exfoliated polymer nanocomposites with improved properties. A variety of polymer characteristics including polarity, molecular weight, hydrophobicity, reactive groups as well as filler characteristics such as charge density and its modified structure and polarity are affective on the intercalation of polymer chains within the filler galleries. Therefore different synthetic approaches have been used for the preparation of polymer nanocomposites. In general there are four preparation methods including insitu template synthesis, solution intercalation, insitu intercalative polymerization and melt intercalation.

In situ template synthesis

In this method the filler layers are synthesized insitu in the presence of polymer chains. The polymer and nanofiller primary precursor are dissolved in an aqueous solution. The gel or slurry is refluxed usually at high temperatures followed by washing and drying. The nucleation and growth of filler layers take place on the polymer chains and the polymer chains are trapped in the filler inter layers.

Solution intercalation

In this method the polymer is dissolved in a solvent and the nanofiller is dispersed in the same solution. The filler is swollen in the solvent and the polymer chains intercalate between the layers. The intercalated nanocomposite is obtained by solvent removal through vaporization or precipitation. Filler can be swollen easily in solvents such as water, acetone, chloroform and toluene. The polymer chains are absorbed onto the delaminated sheets. During the solvent evaporation the entropy gained by the exit of solvent molecules from the interlayer spacing, allows the polymer chains to diffuse between the layers and sandwiching. For example, solution intercalation method is used for the preparation of epoxy /clay nanocomposites [5].

In situ intercalative polymerization

In this method the filler is swollen in monomer liquid or monomer solution. The monomers diffused into the inner layer spacing are polymerized by the heat or radiation, by the diffusion of an initiator or by the initiator present on the modifier of filler. The growth of polymer chains results to the exfoliation and formation of disordered structure. The polarity of monomer and filler layers determines the diffusion rate and equilibrium concentration of monomer. This method is used in the present work.

Melt intercalation

Nanofiller are mixed within the polymer matrix in molten state. The conventional methods such as extrusion and injection molding are used for dispersion of filler layers within the polymer matrix. The polymer chains are intercalated or exfoliated into the galleries. Filler and polymer chains are surface modified with more polar functional groups to enhance their compatibility and therefore promote the exfoliation. In melt intercalation method no solvent is required and it has many advantages for the preparation of nanocomposites and is a popular method for industry. This method is also used in the present work.

1.3.4 Advantages of nanocomposites

Besides their improved properties, these nanocomposites materials are also easily extrudable or mouldable to near-final shape. Since high degrees of stiffness and strength are realized with little amount of high-density inorganic materials, they are much lighter compared to conventional polymer composites. This weight advantage could have significant impact on environmental concerns among many other potential benefits. Thus, it can be considered that nanocomposites have four major advantages over conventional ones:

- Lighter weight of the product due to low filler loading.
- Improved properties (includes mechanical, thermal, optical, electrical etc.) compared with conventional composites at very low loading of filler.
- Larger surface area of nanofillers and combination of specific properties in the composites.

1.4 Nanofiller

Nanofiller is a class of new generation fillers, which have at least one characteristic length scale in the order of nanometer with varying shapes ranging from isotropic to highly anisotropic needle like or sheet like elements. Uniform dispersion of these nanosized particles can lead to ultra-range interfacial area between a polymer and the filler. This poses large interfacial area between the filler and a polymer and nanoscopic dimension differentiate PNC from traditional composites [6]. The major characteristics, which control the performance of nanocomposites, are nanoscale-confined matrix polymer, nanoscale inorganic and organic fillers, and nanoscale arrangement of these constituents [7]. The nanoscale is considered where the dimensions of filler particles (diameter), platelets (thickness) or fibers (diameter) are in the range of 1-100 nm Figure 1.2 [8].

Nanofillers can have different shapes:

- Spherical [e.g., nanosilica, polyhedral pligomeric silsesquioxanes (POSS)]
- Rod / fibre [e.g., synthetic whiskers, carbon nanotubes, sepiolite]
- Sheet / platelet [e.g., layered silicates, synthetic mica etc.]

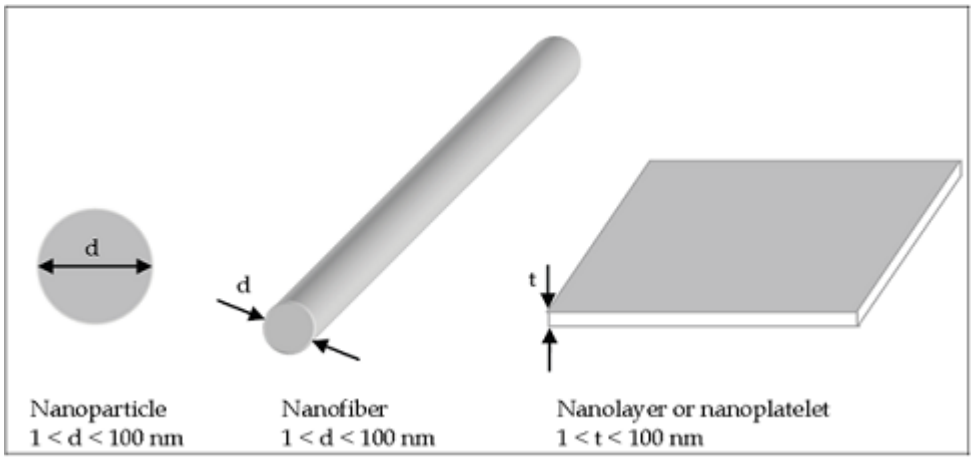

Figure 1.2: Scheme of various types of nanofillers or fillers with nanoscale dimensions

Chapter 2

Literature Review

2.1 Literature search

Rubber has been considered an ideal matrix for nanocomposites[9].

All elastomers have deficiency in one or more properties and blending is a way of obtaining optimum all-around performance [10].

Mishra et al. studied addition of nanofiller along with conventional fillers. With a small size and a large surface area, nanoparticles have many special properties that are different from those of microparticles. However, an improvement in one property can adversely affect another. For optimum properties, nanofillers are an interesting option for today's material research [11].

Polymer nanocomposites have been prepared by various routes, including melt blending [12], in situ anionic intercalative polymerization [13], solution interaction polymerization [14] methods. However, the greatest interest has involved melt processing because this is generally considered more economical, more flexible for formulation, and involves compounding and fabrication facilities commonly used in commercial practice [15]. But among them the most common problem is weak intercalation or poor dispersion of inorganicnanofiller polymer matrix [16].

The synthesis of ordered high performance inorganic/organic polymer nanocoposites (PNs) with a fined tuned structure is a widely investigated reaction because the intimate interactions between composites can provide the enhancement of the bulk polymer properties i.e., mechanical and barrier properties, thermal property, flame retardancy, and abrasion resistance. The large variety of nanoparticles like silica, CaCO3 [11], CNTs [17], POSS [18], metal oxides, Organic clay (a generic name for a whole family of layered aluminosilicate (i.e., montmorillonite)) [19], etc. are of great interest for their unique properties and the high aspect ratio [20].

Reinforcement of a polymer is possible at very low loading of fillers ($<$ 10 wt %) compared to conventional composites, which requires much large quantities. [21], [22].

Nanofillers have a great inclination for agglomeration, because of the high surface energy, especially in polymer melts which is characterized by high viscosity. Therefore, preparation of nanocomposites with uniformly distributed nanoparticles is a challenging task [23].

Polymer-clay nanocomposites possess unique properties because of their nanometer sized features. They can show improved mechanical properties at low filler loading compared to the conventional microcomposites [24].

Novel polymer/clay nanocomposites can be prepared by varying two parameters; first by optimizing polymer to clay ratio and second by varying the processing techniques. An exploration in making the polymer/clay nanocomposites with different clays, surfactants and polymers is a continuing subject of research and interest to both academia and industry [25].

Ray et al. studied that the BR nanocomposites was produced successfully with melt compounding method without a compatibilizer, unlike with other hydrophobic polymers such as polypropylene and polyethylene. The intercalation of BR into the organoclay was evident from X-Ray Diffraction (XRD) and was confirmed by Transition Electron Microscopy (TEM) study [26].

Kim et al. reported that the tensile and tear strength of the BR/ Cloisite 20A hybrids were improved, rebound resilience, compression set, and abrasion resistance were also improved by the addition of organoclay. To produce the same mechanical strength as in polymer 3-5% silicate nanocomposites, 30-60% filler has to be incorporated in conventional composites. Therefore, rubber/ organoclay nanocomposites can make much lighter rubber parts with improved elastic properties over conventional composites [27].

Chaoying et al. prepared intercalated BR/Clay nanocomposites by direct melt compounding. They found that the intercalation occurred in the compounding process and that the intercalation degree was further enhanced by vulcanization [28].

Varghese et al. reported that the clay modified with primarily ammonium and quaternary ammonium compounds (DDACs) creates different microstructure in a sulphur-cured polar rubber matrix, such as hydrogenated nitrile rubber [29], and epoxidized NR [30].

Chaoying et al.studied that the tensile strength, elongation at break, and tear strength of the BR/Clay/DDAC vulcanizates were greatly improved in comparison with those of the gum BR and BR/pristine clay vulcanizates but were somewhat lower than those of BR/organoclay vulcanizates [28], [31], [32].

Unique Rheological behaviour of BR/Clay nanocomposites was studied by Bhowmik et al. and they found out that the nanocomposites show shear thinning, i.e. the shear viscosity decrease with increasing shear rate following power law. The shear viscosity and die-swell decrease with addition of the nanoclay [33].

Carbon nanotubes (CNTs) are unique nanostructured materials with remarkable physical, mechanical, and electronic properties. These properties make them attractive for applications in many scientific and technological fields such as electronic structures, polymer composites, and biological systems [34].

Kovalchuk et al. reported that a single nanotube is hundred times stronger and six times lighter than steel and exhibits good electrical and thermal conductivities [35]. Polymer and CNTs can interact in several ways such as (a) physical adsorption of macromolecular chains on the surface of the CNTs, (b) chemical interaction between polymer and CNT surface via some interacting functional groups, (c) covalent carbon–carbon linking, (d) ionic interactions through cation electron transition and (e) mechanical chain entanglements [36].

Das et al. reported that as far as rubbery polymers are concerned, insufficient dispersion (due to high viscosity of the rubbery polymer and poor interactions between elastomers and CNTs) of CNTs leads to elastomeric composites with low performance properties. Homogeneous distribution and good dispersion of the CNTs have been a potent challenge in rubber composites [37].

Pompeo et al. studied that multi-walled carbon nanotube (MWCNT) along with an ionic liquid 1-allyl-3methyl imidazolium chloride (AMIC) provide a strong level of reinforcement to an SBR/BR rubber matrix. The chemical coupling between carbon nanotubes and rubber chains by AMIC is evidenced by Raman spectra, dynamic mechanical analysis, and electrical properties [38].

Since the 1990s, silica particles have been studied as tire fillers to improve tire properties such as rolling resistance, wet grip, and abrasion resistance [39], [40]. However, when pure silica particles are mixed with rubber, the silica easily agglomerates due to the strong filler-filler interaction resulting in poor mechanical, optical, and electrical properties. This is because rubber generally demonstrates hydrophobic properties. Therefore, the surface characteristics of silica should be modified from hydrophilic to hydrophobic to avoid silica agglomeration in rubber-silica composites [41], [42].

A novel class of fillers are nanosilica and nanoclay which attains unique properties. In contrast to silica fillers in polymer matrices where matrix-filler and filler-filler interaction can be controlled by surface modification with silanes, in nanosilica having fine particles size distribution is generated in situ through the mixing process which results to change aggregate structure. The second feature of the nanosilica is their anisotropic nature which leads to filler networking at much lower loading levels than for isotropic carbon black or silica or clay fillers [43].

Arun et al. reports that lesser amount of nanosilica (0.6phr of 20% nanosilica dispersion) is only required for the better mechanical properties compared to the amount of silica (up to 10 phr of 40% silica and the effects of nanolayer reinforcement are also manifested in terms of reduced swelling by solvents, and higher modulus values [44].

Zang et al. and Guo et al. studied that good bonds between nanoparticles and the polymer is still a challenge for specific nanocomposites fabrication. However, appropriate chemical engineering treatment (functionalization) of the nanofiller surface by introducing proper functional groups could improve both the strength and toughness of the composites with improved compatibility between the nanofillers and the polymer matrix [45], [46].

The performance of rubber composites filled with nanosilica has been improved by surface modification of the nanosilica using silane coupling agents. The bonding force and dispersion of nanosilica in rubber were thus significantly improved. Also the physical and mechanical properties of the vulcanized rubber were greatly improved [47], [48], [49], [50].

Nanosilica powder has been modified with silane coupling agents, 3-(2 aminoethyl) - amino-propyl trimethoxy silane and bis[3-(triethoxysily)- propyl] disulfide, and applied to formulations with solution polymerized styrene butadiene rubber. Compared with SBR filled with silica powder, SBR filled with silica powder modified by a silane coupling agent exhibite not only better filler dispersion and mechanical properties, but also lower internal friction loss over a selected range of strains [51].

Bhowmik et al. proposed that the diffusion of solvents on polymer nanocomposites depends on (a) the geometry of the dispersed phase (shape, size, and size distribution and orientation); (b) properties if dispersed phase; (c) properties of continuous phase and (d) interaction between the polymer and the nanofiller. In the polymer/clay nanocomposites permeability decreases significantly with the addition of only 4 phr of the unmodified montmorillonite clay (0.14×10^{-8} cm^2 s^{-1}) compared with that of neat polymer (2.29×10^{-8} cm^2 s^{-1}) [52].

In situ methods can create strong chemical bonding within the nanocomposites and are expected to produce a more stable and higher quality nanocomposite [53].

PI, BR and SBR nanocomposites have been successfully synthesised by in situ anionic intercalation polymerization. The XRD and TEM results reveal that a certain extent of exfoliated nanocomposites can be prepared by this process [13], [28], [54].

1, 3-Butadiene undergoes stereospecific polymerization to high molecular weight cis-1, 4-polybutadiene (>97% cis-1,4 content) in presence of soluble catalysis comprising cobalt (II) salts and diethylaluminium chloride was reported by Upadhayay et al. In spite of the widespread use of this chemistry in industrial practices, little systematic information is available in the literature [55].

Pires et al. reported that 1,3-Butadiene undergoes stereospecific polymerization to high molecular weight cis-1,4-polybutadiene (>97% cis-1,4 content) with four different technologies with Ziegler-Natta catalysts can be used in the commercial production of BR. Titanium (Ti), Cobalt (Co), Nickel(Ni) and Neodymium (Nd) are the most commonly used metals in these catalyst system [56]

Leo et al. presented a general scheme to explain in a quantitative and qualitative manner various features of Ziegler-type polymerization such as (1) the dependence of polymerization rate on monomer concentration, (2) the dependence of rate on aluminium alkyl, (3) dependence of rate on catalyst ratio, (4) the factors upon which molecular weight depended, (5) the effect of temperature on molecular weight, (6) the effect of temperature on polymerization rate, (7) the stereospecific polymerization aspects [57].

Natta et al. reported that the Diethylaluminium Chloride (Et2AlCl) in combination with cobalt catalyst requires water in a certain mole ratio to the Diethylaluminium Chloride (DEAC) to activate when Water/ Aluminium (W/Al) ratio is varied in certain range [58].

The nature of solvents employed in polymerization plays a definitive role in determining the polymerization rate, polymer molecular weight and its microstructure. The most commonly used solvents are benzene and toluene. However, aliphatic solvents such as n-hexane, n-heptane or cyclohexane are also used. [59], [60], [61], [62].

However, there is no reported work on synthesis of BR nanocomposites by in situ method using Ziegler-Natta catalysts.

2.2 Scope and objectives

In 1978, IPCL Vadodara, now Reliance Industries Ltd-Vadodara Manufacturing Division (RIL-VMD) established PBR-I manufacturing facility with the know-how from Polysar Canada. The installation capacity of this plant is 20,000 TPA; later in 1996, IPCL (RIL-VMD) set up another plant with know-how from Japan Synthetic Rubber Co. Ltd, Japan. The installed capacity of this plant is 40,000 TPA. Both the plants use different solvent and catalyst system.

Polybutadiene rubber (BR) accounts for approximately 25% of the world's production of synthetic rubber. Seventy percent of total production is used in tire compounds, with another twenty percent being used for production of soles, gaskets, seals, belts, etc. Until now, there has been very little information available regarding BR/Nanocomposites (NCs) because hydrophobic polymers, such as polypropylene, polyethylene and polybutadiene are very difficult to use for creating nanocomposites without a compatibilizer.

Even today carbon black continues to be the most important reinforcing agent in the rubber industries. About 5 million metric tons of carbon black is globally consumed each year. But, due to its polluting nature, black colour of the compounded rubber material and its dependence on the petroleum feedstock (for synthesis) caused researchers to look out for other "environment friendly, white, light weight and cheap reinforcing agents" or combination of these properties.

The synthesis of ordered high performance inorganic/organic polymer nanocomposite is widely investigated. It is defined as heterogeneous mixture of two or more materials, a continuous phase, termed as the matrix, and a reinforcing agents or fillers which are dispersed on nanolevel. Nanocomposites can provide the enhancement of the bulk polymer properties i.e., mechanical and barrier properties, thermal property, flame retardency, and abrasion resistance with variety of non black and pollution free nanoparticles like nanosilica, layered nanosilicates, synthetic mica, sepiolite, CaCO3, etc.

Silica has a number of hydroxyl groups on the surface, which results in strong filler-filler interactions and adsorption of polar materials by hydrogen bonding since intermolecular hydrogen bonds between hydroxyl groups on the surface of silica are very strong and it can form a tight aggregate. The aggregation leads to the formation of a weak point on the matrix and consequently reduces the mechanical properties. The solution of this problem lies in the

use of silane coupling agent, which shields the polar silica surface on one hand and reacts with the rubber matrix on the other hand.

Until now, BR nanocomposites have been prepared by various routes, including melt intercalation and solution blending, but among them the most common problem is weak intercalation or poor dispersion of nanofillers in organic compounds. In situ polymerization method for preparation of BR nanocomposites may be the solution of this problem because of better nanofiller dispersion.

Hence, objective of this thesis are to improve the performance of BR/nanocomposites in terms of physico-mechanical properties, thermal and swelling properties as well as to get the exfoliated structure by using nonconventional filler (Nanosilica, Nanosilica+10% Silane coupling agent, CNT, Cloisite-20A, Cloisite-30B, Pangel-B20, etc.). Literature search shows that BR nanocomposites are mostly prepared using solution or melt blending method. However in this project, nanofillers will be incorporated through melt compounding which is commercially viable and environment friendly process and in situ polymerization process to overcome the problem of weak interaction and/or bad dispersion.

2.3 Project Layout

1. To evaluate the effect of different nanofillers on the physico-mechanical properties of BR by *ex situ*/melt blending.
    - Nanofillers used: Cloisite 20A, Cloisite 30B, Pangel B20, CNT, Nanosilica, Nanosilica-silane and hydrotalcite.
    - Optimization of filler loading.
    - Characterization of the nanofillers and nanocomposites.
2. Selection of most effective nanofiller, based on physico-mechanical properties.
3. Evaluate the thermal properties (TGA-DSC) and characterization (XRD) of optimized nanocomposites.
4. Establishment of structure-property relationship in optimized BR nanocomposites.
5. Comparison of physico-mechanical properties of BR nanocomposites (CNT and nanosilica) with non conventional BR composites (Carbon black and precipitated silica).
6. Synthesis of *in situ* BR nanocomposites
    - Nanofiller used: CNT, Nanosilica, Cloisite 20A and Cloisite 30B
7. Establishment of structure-property relationship in *in situ* BR nanocomposites.
8. Studies on swelling behaviour of BR nanocomposites.
9. Comparison of optimized BR nanocomposites produced by melts blending (*ex situ*) and *in situ* polymerization method on the basis of physico-mechanical properties.

Chapter 3

Experimental

3.1 Materials

The materials used for this study are as given in Table 3.1.

Table 3.1: Materials used for this study

Materials	Supplier	Function
Polybutadiene Rubber (BR)	RIL, India	Rubber (Elastomer)
CLOISITE 20A	Southern Clay, USA	Nanofiller
CLOISITE 30B	Southern Clay, USA	Nanofiller
PANGEL B20	Tolsa, Spain	Nanofiller
Multi walled CNT	Aldrich, USA	Nanofiller
Nanosilica	Labort, India	Nanofiller
Mg/Al & Zn/Al Hydrotalcite	Synthesized in RIL	Nanofiller
Carbon Black	Philips Carbon Black	Reinforcing filler
Precipitated Silica	Labort, India	Reinforcing filler
Sulphur	Labort, India	Crosslinking agent
CBS	Labort, India	Accelerator
Stearic acid and Zinc oxide	Labort, India	Activator
3-Aminopropyl-trimethoxylane	Aldrich, USA	Coupling agent
Wax	Labort, India	Antiozonant
6PPD	John Baker, USA	Antioxidant
Cobalt Octoate	PBR I, RIL-VMD	Catalyst
Diethyaluminium chloride	PBR I, RIL-VMD	Co-Catalyst
Water	-	Promoter
Cyclohexane	Labort, India	Solvent system
1,3-Butadiene	PBR II, RIL-VMD	Monomer
Methanol	Labort, India	Terminator

3.2 Preparation of BR nanocomposites

Two process routes have been followed by us for preparation of BR nanocomposites in our-work, they are *ex situ* and *in situ* polymerization method. In the first process BR nanocomposites are made by melt compounding in our laboratory, detailed process description for this is given in the following section. In *in situ* process the 1, 4-polybutadiene rubber is produced within the laboratory, this gives us an advantage that we can add the nanofillers inside the reaction mixture itself. It is expected to get intercalated or exfoliated structures of nanocomposites by this activity. Other chemicals are added to this rubber by melt compounding method same as ex situ process.

3.2.1 *Ex situ* / Melt compounding

A conventional compounding system is used for melt compounding. Table 3.2 shows the composition of the rubber compounding. The master batch (MB) preparation is done by using Plasti-Corder (Brabender Duisburg, Germany) at 40 rpm and 145 °C for 10 min. Curatives are mixed into the MB by using a two-roll mill at 60 ± 5 °C for 5 min.

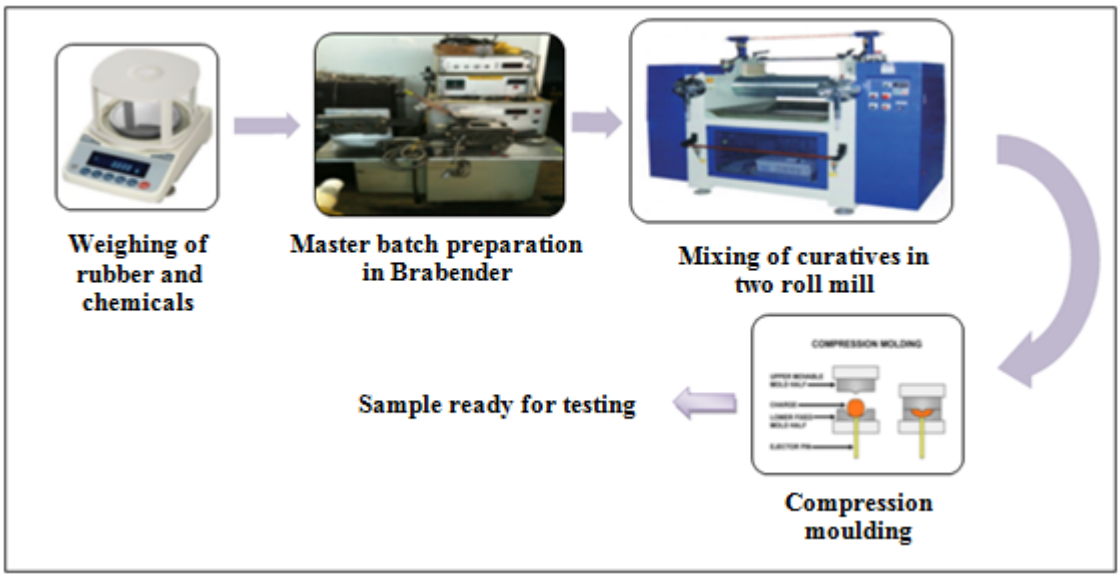

Figure 3.1: Sequence of composites preparation

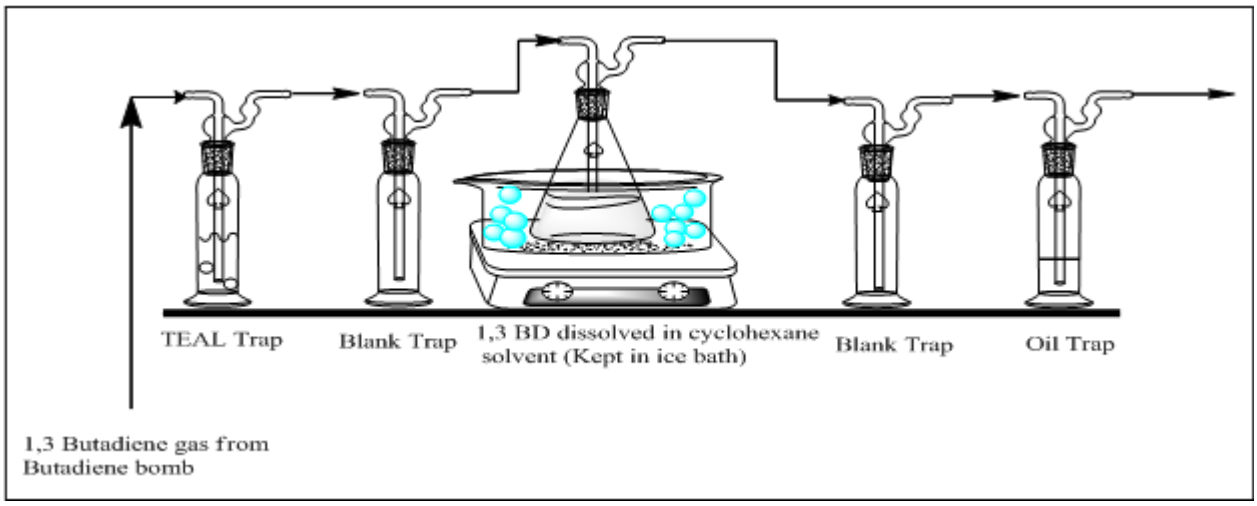

Figure 3.2: Schematic diagram of feed preparation

3.2.2 *In situ* polymerization

To get dry BR nanocomposites by *in situ* polymerization following steps are followed.

Feed preparation:

Schematic diagram of feed preparation is shown in Figure 3.2. 1, 3-Butadiene is bubbled through traps containing 8% solution of Triethylaluminium (TEAL) in toluene followed by blank trap. Then it is is dissolved in pre-weighed solvent cyclohexane in flask, which is kept in the Ice-bath. Theinsoluble 1, 3-Butadiene gas is passed through blank trap followed by oil trap. The ratio of monomer to solvent is kept about 20:80.

Polymerization:

Reactor assemblys are shown in Figure 3.3. Both systems have been used as per the amount of feed taken for polymerization. Buchi reactor is used for capacity between 250 to 300 gm. of feed and for 100 to 200 gm. of feed three necked flask system has been used. Polymer.

Recovery:

As the reaction proceeds, the reaction mass becomes viscous and this is the indication of polymer formation. Polymerization is terminated with methanol containing 0.5% of di-tert-butyl-para-cresol (DTBPC). Rubber comes out of the solution when methanol is added. Then rubber is separated by decantation. Sample.

Drying: The sample is kept on a plastic dish in fuming hood at room temperature for one day. Then it is cut in small pieces. Sample is placed in a vacuum oven at 45°C for 6 hr

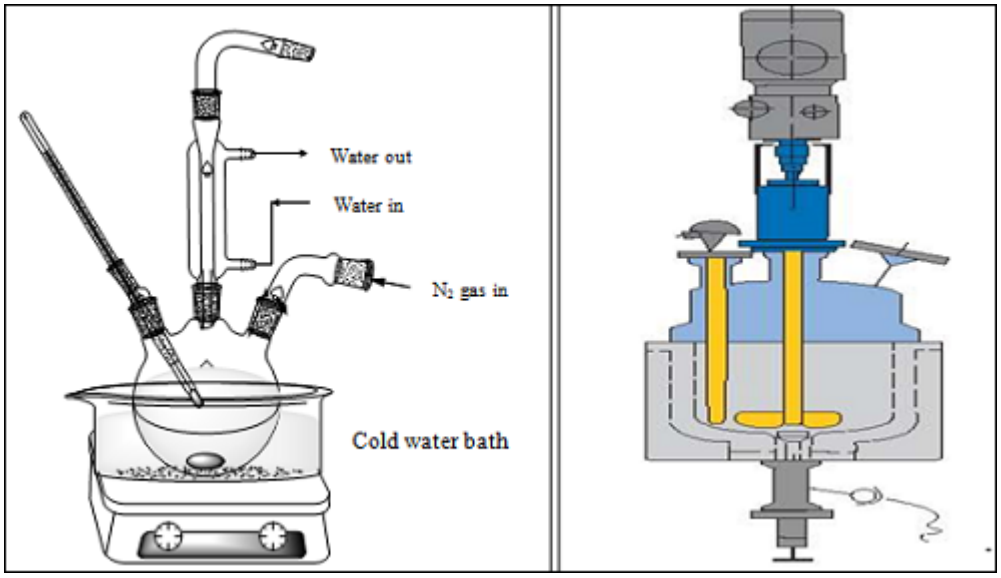

Figure 3.3: Schematic diagram of reactor assembly

3.3 Curing

Curing of compounding is performed by compression-moulding machine (Pathex, Canada) in a simple still-plated mould with dimensions of 150mm x 150mm x 3mm. The samples are compressed under 4 kg/cm^2 of pressure at 145 °C for curing for optimum time.

3.4 Specimen preparation

Most physical tests on vulcanizates are performed on specially prepared samples. Different maturation periods after mixing, after remilling, and after curing are required for compounds based on different polymers. In general, no tests should be conducted till at least 16 hours after vulcanizing a sample because significant post-vulcanization changes in structure of the material occur during this period.

3.5 Characterization

3.5.1 Cure characterization

Instead of curing each test compound at separate ranges of temperatures and making separate tensile tests,cure meter is used. In this instruments modulus changes is monitored during the

Table 3.2: Table 3.2: Formulation and designation of different rubber composites

Material	Formulation in phr									
	BR	BR/CNT	BR/20A	BR/30B	BR/B20	BR/ nanosilica	BR/nanosilica-silane	Mg-Al HT & Zn-Al HT	BR/CB	BR/ Silica
BR	100	100	100	100	100	100	100	100	100	100
Wax	0.7	0.7	0.7	0.7	0.7	0.7	0.7	0.7	0.7	0.7
6PPD	1	1	1	1	1	1	1	1	1	1
Stearic acid	0.7	0.7	0.7	0.7	0.7	0.7	0.7	0.7	0.7	0.7
Zinc oxide	1.7	1.7	1.7	1.7	1.7	1.7	1.7	1.7	1.7	1.7
MWCNT		1,3,5,8								
Cloisite 20A			1,3,5,8							
Cloisite 20B				1,3,5,8						
Pangel B20					1,3,5					
Nanosilica						1,3,5	1,3,5,8			
Silane							10 wt % of nanosilica			
Mg-Al & Zn-Al								1,3,5		
CB									1,3,5,8	
Precipitated silica										1,3,5
Oil	1.7	1.7	1.7	1.7	1.7	1.7	1.7	1.7	1.7	1.7
Sulphur	0.7	0.7	0.7	0.7	0.7	0.7	0.7	0.7	0.7	0.7
CBS	0.7	0.7	0.7	0.7	0.7	0.7	0.7	0.7	0.7	0.7

cure. Compound cure characteristics are measured on Oscillating disc rheometer (Monsanto ODR 2000, USA) as per ASTM D2084-95. The testing is performed at 145 ℃ for 1 hr. An envelop of a typical cure curve is given in Figure 3.5.

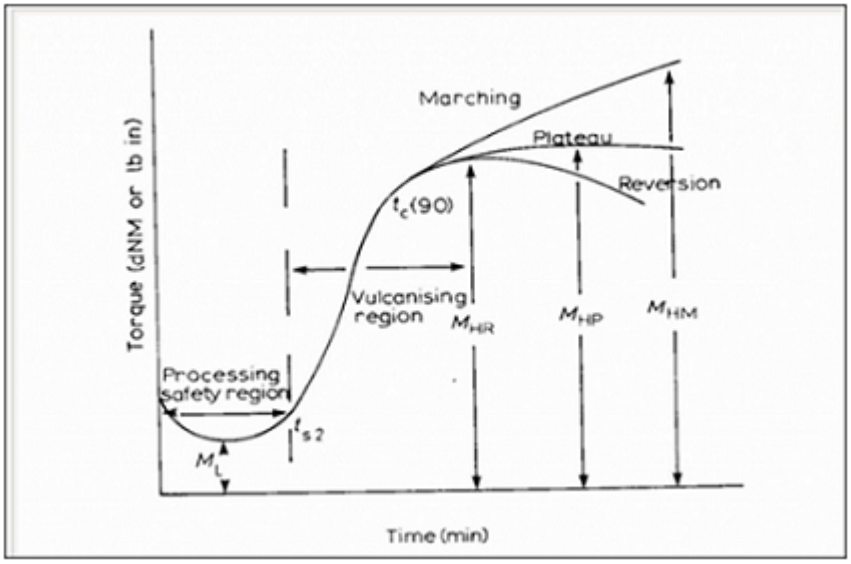

Figure 3.4: A typical rheograph, explaining optimum cure time

3.5.2 X-ray diffraction (XRD) Analysis

XRD is the powerful tool for structural characterization. It is well known that x-ray diffraction method can be applied to identify the microstructural interfacial interaction, degree of crystallization of the polymer nanocomposites. X-ray diffraction is performed by equipment model (Bruker D8 Advance, Germany) on the BR nanocomposites samples and also the pure filler samples at the Cu Kα wavelength of 1.5406 Å. The diffracogram (2ϑ) is scanned in range from 1 to 90°.

XRD is a non-destructive technique that reveals detailed information about the chemical composition and crystallographic structure of materials. It is based on Bragg's law.

$$\eta\lambda = 2d\sin\theta \tag{3.1}$$

3.6 Test methods

3.6.1 Tensile Properties

The stress-strain test in tension, including ultimate tensile and elongation, is probably still the most widely used test in the rubber industry. Among the purposes for such tests are: to ensure that all compounding ingredients have been added in the proper proportions, to

determine rate of cure and optimum cure for experimental polymers and compounds, for specification purposes, and to obtain an over-all check on the compound.

Tensile properties are determined on a universal testing machine (model Instron-3366, UK). Testing is performed at room temperature. Tensile strength (TS), Modulus (MOD) at 100% and 300% elongation and % elongation at break (%EB) are determined at a deformation speed at 500 mm/min. The mean value of three measurements is reported here. The tensile properties are reported as per ASTM D412-00.

3.6.2 Hardness

Hardness, as applied to rubber, may be defined as the resistance to indication under conditions which do not puncture the rubber. The compression-moulded specimens (6 mm thickness) are tested to determine the hardness data with an International Rubber Hardness Dura meter (Wallace Test Equipment, England) as per ASTM D2240-05.

3.6.3 Crosslink density

In polymer science, Flory–Rehner equation is an equation that describes the mixing of polymer and liquid molecules as predicted by the equilibrium swelling theory of Flory and Rehner. It describes the equilibrium swelling of a lightly crosslinked polymer in terms of crosslink density. Swelling wasis determined according to ASTM D471-12, which is calculated by equation 3.2.

$$\nu = -\frac{ln(1 - Vr) + Vr + xVr^2}{Vs(Vr^3 - 0.5Vr)} \tag{3.2}$$

3.7 Thermal analysis (TGA - DTG)

TGA is done using Thermogravimetric analyzer from TA Instruments (SDT Q600 V20.9) at heating rate of 10°C per min in N2 atmosphere.

TGA measures the amount and rate of change in the weight of a material as a function of temperature or time composition of materials and to predict their thermal stability at temperature up to 800°C. TGA can characterize materials that exhibit weight loss or gain due to decomposition, oxidation or dehydration.

3.8 Solvent resistance

Swelling experiments are performed by placing the previously weighed test samples into the solvent (toluene) containers (gram of sample versus volume of liquid 1:100). At periodic intervals, the test samples are removed from the solvent container and the extra solvent on the surface is wiped quickly with blotting paper and the samples are weighed immediately. After weighing, the samples are placed back in to the same container. After equilibrium swelling, the samples are deswollen. For deswelling, the swollen samples are kept in air until they reach a constant weight. It takes around 6 hr. to evaporate off the absorbed solvent completely at 30°C.

Chapter 4

Results and Discussions

4.1 Characterization of filler

Six types of fillers in BR compound are used in the present work. The particle size and the Brunauer–Emmett–Teller (BET) surface area of these fillers are reported in Table 4.1. It has been already reported in the literature that higher the surface area, higher will be the reinforcement. From Table 4.1, nanofillers are expected to show better reinforcement.

Table 4.1: surface area of different filler

Sample	CB	Precipitated Silica	CNT	Nanosilica	Cloisite 20A and 30B	Pangel B20
Particle size	o.d. : 30-35 nm	2-7 μm	o.d. x l : 6-9 mm x 5 μm	5-10 nm	2 μm	5-8 μm
Surface area (m^2/g)	74	< 80	450-500	490-500	150-175	115

Different composites are prepared using four different groups of nanofillers, eg., organo nanoclay, nanosilica, hydrotalcite and carbon nanotubes.physico-mechanical properties of nanocomposites made of each group of nanofillers have been discussed in the following reactions.

4.2 Effect of organo nanoclay on BR based nanocomposites

The physico-mechanical properties of the BR organo nanoclay hybrids are shown in table 4.2. Remarkable increments in the mechanical properties are seen for the BR organo nanoclay hybrids.

Table 4.2: Mechanical properties of the BR/ organofiller nanocomposites

Sample	T.S (MPa)	EB %	300% MOD (MPa)	100% MOD (MPa)	Hardness	Crosslink density X E-05
BR	1.66	302	1.09	0.68	41.0	3.35
BR/Cloisite 20A-A	3.52	909	1.09	0.66	50.0	4.42
BR/Cloisite 20A-B	5.72	966	1.18	0.68	58.0	5.02
BR/Cloisite 20A-C	4.44	989	1.18	0.60	56.5	4.09
BR/Cloisite 20A-E	3.12	185	1.98	0.98	55.0	4.15
BR/Cloisite 30B-A	3.11	915	1.09	0.64	52.0	3.26
BR/Cloisite 30B-B	4.06	877	1.40	0.70	57.0	2.75
BR/Cloisite 30B-C	3.64	667	1.28	0.68	54.0	1.99
BR/Cloisite 30B-E	3.02	226	0.99	0.54	57.5	2.02
BR/Pangel B20-A	3.27	761	1.36	0.67	54.5	4.25
BR/Pangel B20-B	2.37	682	1.04	0.59	54.0	3.52
BR/Pangel B20-C	2.22	648	1.21	0.67	55.0	3.69

For the **BR/Cloisite 20A (3 phr)** nanocomposite, Tensile strength and Elongation at break has improve by 245% and 220% respectively as compared to gum BR vulcanizate. Hardness and Crosslink density has also improve by 41% and 50% respectively as compared to BR. The relationship of the filler loading with tensile properties of BR/Cloisite 20A is shown in Figure 4.1. Both TS and EB show a maxima and their decrease with increasing filler loading. The plausible reasons for such behaviour are discussed in the section 4.6.

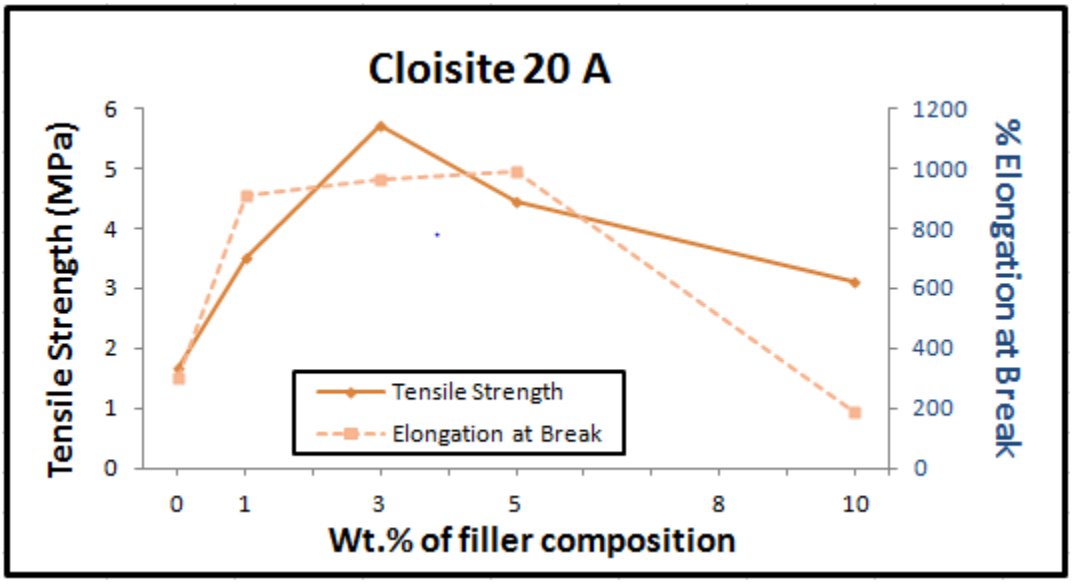

Figure 4.1: Effect of Cloisite 20A loading on tensile properties of BR composites

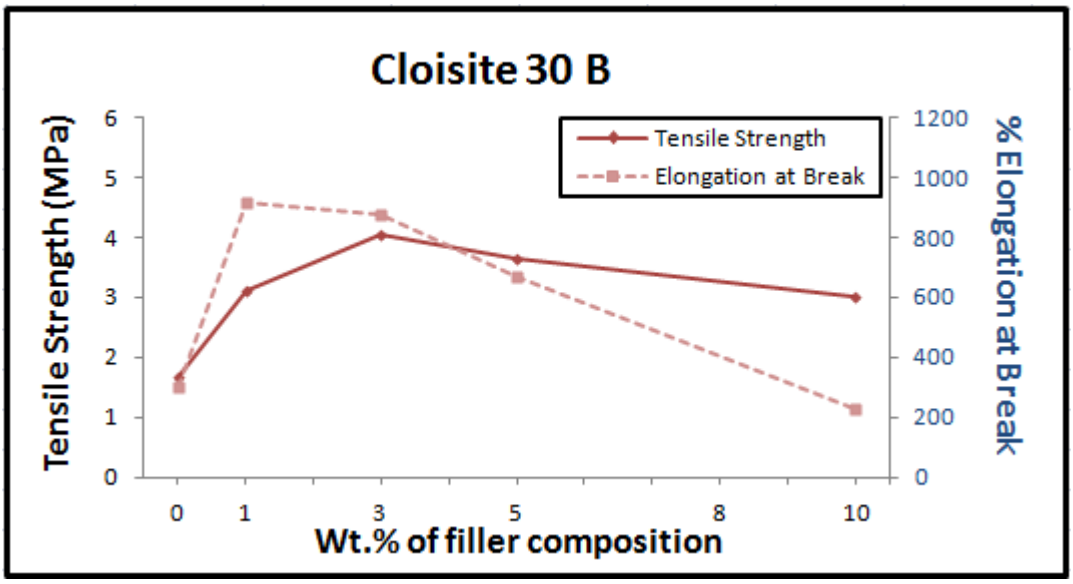

Figure 4.2: Effect of Cloisite 30B loading on tensile properties of BR hybrids

For the **BR/Cloisite 30B (3 phr)** nanocomposite, TS and EB has improve by 145% and 190% respectively as compared to BR vulcanizates. Hardness has also improved 39% as compared to BR. The relationship of the filler loading with tensile properties of BR/Cloisite 30B is shown in Figure 4.2. TS is maximum at 3 phr and then flattens EB goes through peak in the 1-3 phr loading and then decrease. The behaviour is explained in the section 4.6. For the **BR/Pangel 20B (1 phr)** nanocomposite, TS and %EB has improved 97% and 152% respectively as compared to BR. Hardness and Crosslink density has also improved 33% and 27% respectively as compared to BR.

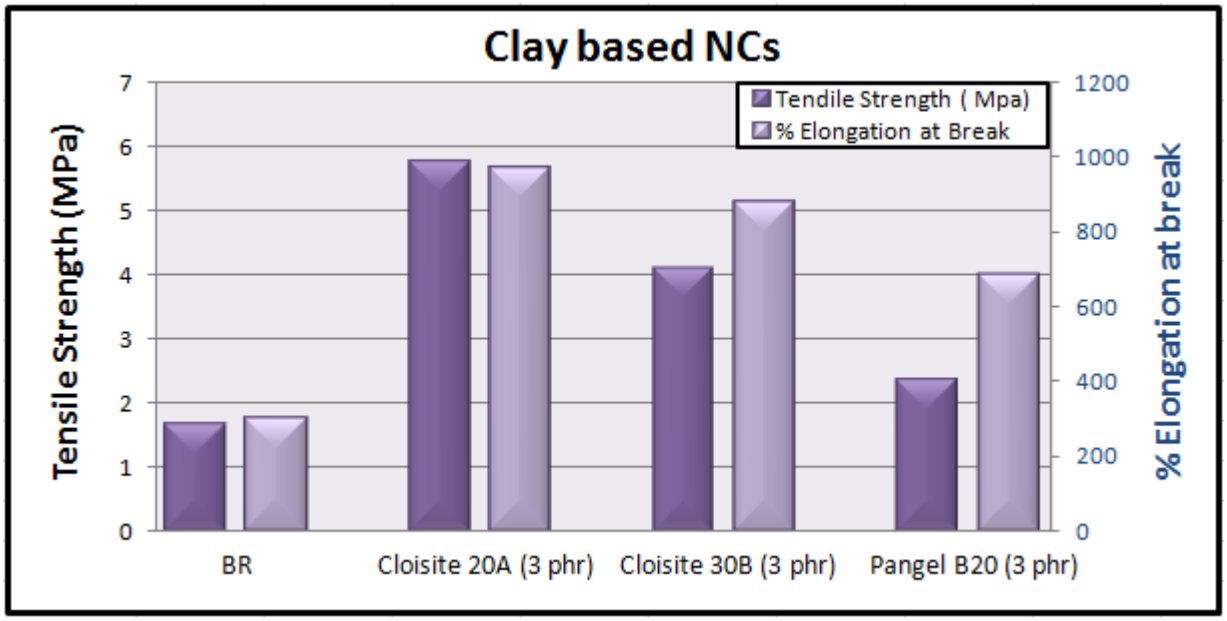

Figure 4.3: TS and %EB of 3 phr BR/ Clay based NCs

The above results tell that the BR/Cloisite 20A nanocomposites possess the highest physico-mechanical properties followed by BR/Cloisite 30B nanocomposites at 3 phr filler loading, where as BR/Pangel 20B nanocomposites are not much affected. With the increasing filler loading properties decrease in all the samples. This is due to intercalated-exfoliated structure at 3 phr and agglomeration of filler at higher loading, and which is also confirmed by X-Ray Diffraction (XRD) results in section 4.6. The comparison of TS and EB of BR NCs filled with Cloisite 20A (3 phr), Cloisite 30B (3phr) and Pangel B20 (3phr) is shown in Figure 4.3.

4.3 Effect of Hydrotalcite on BR nanocomposites

The physico-mechanical properties of the BR/activated hydrotalcite NCs are reported in table 4.3. Increments in the mechanical properties are seen for the BR/activated Mg-Al-HT and BR/activated Zn-Al-HT NCs.

Table 4.3: Physico-mechanical properties of the BR/activated hydrotalcite nanocomposites

Sample	T.S (MPa)	EB %	300% MOD (MPa)	100% MOD (MPa)	Crosslink density X E-05
BR	1.66	302	1.09	0.68	3.35
Zn-Al-HT-A	1.33	390	1.06	0.62	40.3
Zn-Al-HT-B	2.66	614	1.51	0.69	4.13
Zn-Al-HT-C	1.83	436	1.34	0.74	4.50
Mg-Al-HT-A	2.29	530	1.52	0.91	3.13
Mg-Al-HT-B	2.92	860	1.33	0.97	4.08
Mg-Al-HT-C	1.73	386	1.36	0.72	4.75

For the **BR/activated Mg-Al hydrotalcite (3 phr)** nanocomposite, TS and EB has improve by 76 % and 185 % respectively and for 100 and 300% modulus, 43% and 20% improvement is recorded respectively as compared with gum BR vulcanizates. Crosslink density has improve by 22% as compared to BR, and also gradual improvement is seen by further filler loading. The same kind of trend is observed for the **BR/activated Zn-Al hydrotalcite (3 phr)** nanocomposite, TS and EB has improve by 60% and 103% respectively as compared to BR . Crosslink density improve by 23% as compared to BR, and also gradual improvement seen by further filler loading. The relationship of the tensile properties with filler loading of Activated Zn-Al hydrotalcite and Activated Mg-Al hydrotalcite are shown in Figure 4.4.

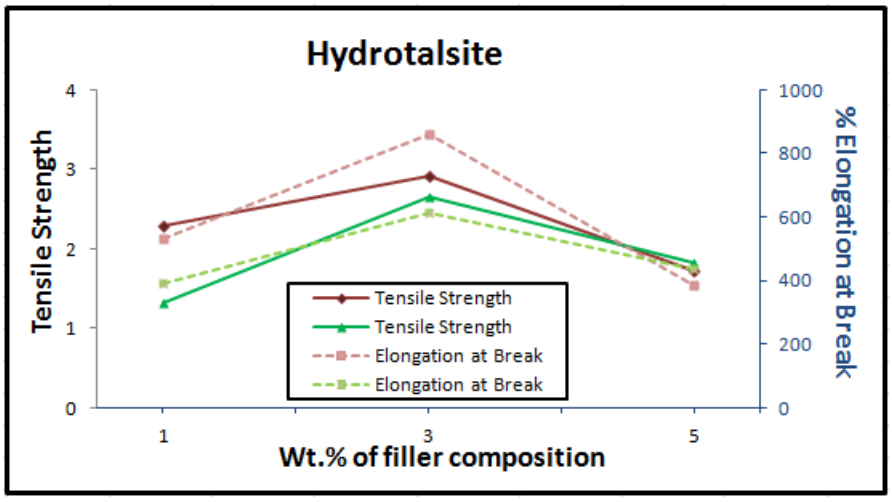

Figure 4.4: Effect of filler loading on tensile properties of BR/ activated Mg-Al-HT and BR/activated Zn-Al-HT NCs

4.4 Effect of nanosilica on BR based nanocomposites

Different physico-mechanical properties of nanosilica composites are reported in Table 4.4. Silane coupling agents are used to improve polymer-filler interaction. Effect of silane coupling agent (3-Aminopropyl-trimethoxylane) on nanosilica is discussed in this section. The nanosilica loading has been varied as 1, 3 and 5 phr with a constant loading of silane (10 wt % filler).The relationship of the tensile properties with filler loading of nanosilica-silane NCs are shown in Figure 4.5. For **BR/nanosilica-silane (3 phr)** nanocomposite, an improvement of 124% and 113% is observed respectively in TS and EB and for 100 and 300% MOD, 65% and 22% improvement is recorded respectively as compared to gum BR vulcanizates. Crosslink density has also improve up to 27% than that of BR/nanosilica-B. Further filler loading in this case decreases the property due to agglomeration.

Table 4.4: Physico-mechanical properties of the BR/nanosilica nanocomposites

Sample	T.S (MPa)	EB %	300% MOD	100% MOD	Hardness	Crosslink density
BR	1.66	302	1.09	0.68	41.0	3.35
BR/ Nanosilica-A	2.04	302	0.94	0.61	50.0	3.06
BR/ Nanosilica-B	1.17	648	1.01	0.61	53.5	3.33
BR/ Nanosilica-C	1.43	371	0.97	0.62	51.0	2.32
BR/ Nanosilica-Silane-A	1.71	590	1.01	0.69	51.0	3.56
BR/ Nanosilica-Silane-B	3.72	642	1.80	0.83	55.0	4.22
BR/ Nanosilica-Silane-C	2.36	580	1.22	0.63	53.0	3.57

Table 4.5: Physico-mechanical properties of the BR/CNT nanocomposites

Sample	T.S (MPa)	EB %	300% MOD (MPa)	100% MOD (MPa)	Hardness	Crosslink density X E-05
BR	1.66	302	1.09	0.68	41.0	3.35
BR/ CNT-A	1.86	523	1.08	0.60	50.0	3.72
BR/ CNT-B	2.31	447	1.39	0.74	53.0	4.89
BR/ CNT-C	3.93	432	2.66	1.07	54.0	4.24
BR/ CNT-D	3.33	386	2.86	1.19	54.4	4.31
BR/ CNT-E	2.97	199	2.63	1.29	54.0	6.02

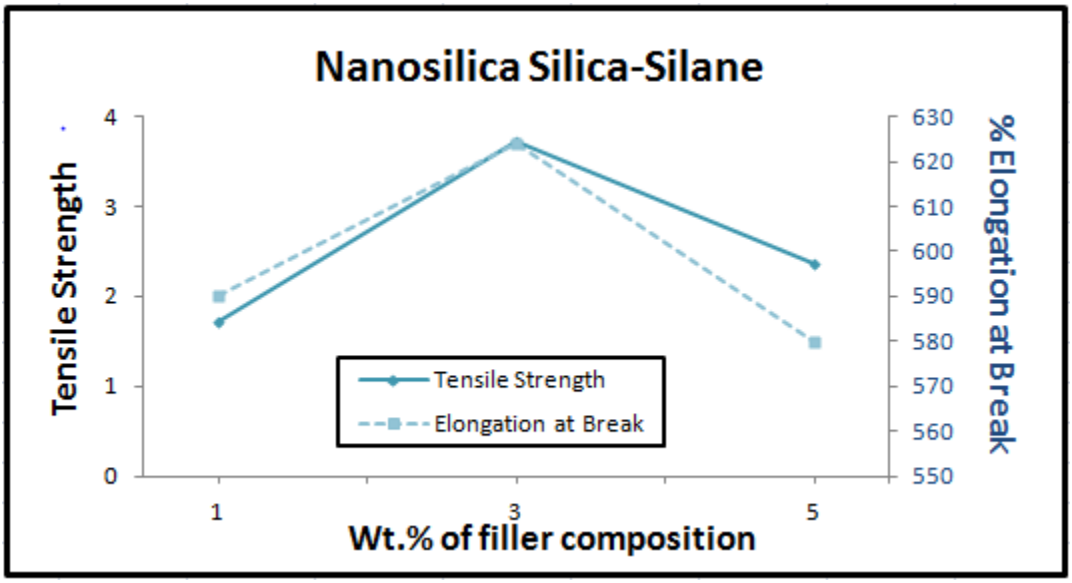

Figure 4.5: Effect of filler loading on tensile properties of BR/Nanosilica-Silane NCs

4.5 Effect of CNT on BR nanocomposites

Different physico-mechanical properties of CNT nanocomposites are reported in Table 4.5. For the BR/CNT NCs, a remarkable improvement in the mechanical properties has been obtained. Improvement in TS and EB of **BR/CNT (5 phr)** nanocomposite improve by 137% and 43% respectively and 144% and 57% increament is observed in the case of 100 and 300% modulus respectively compared to gum BR vulcanizates. Hardness has also improved up to 32% compare to BR, but with further filler loading TS and EB gradually decrease. The relationship of the filler loading with tensile properties of BR/CNT is shown in Figure 4.6. The crosslink density has also improve with addition of CNT compared to BR.

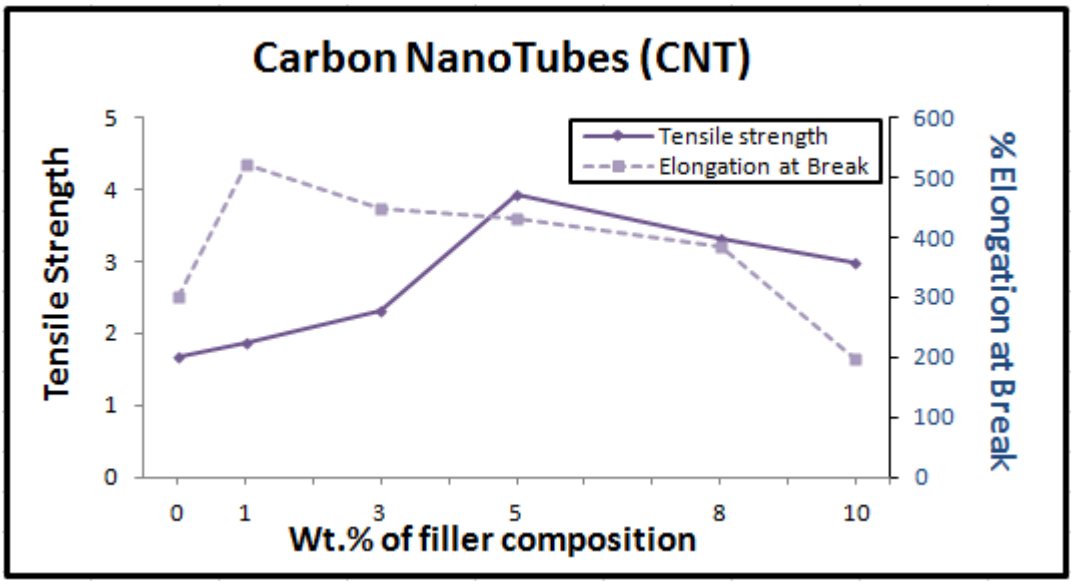

Figure 4.6: Effect of filler loading on tensile properties of BR/CNT NCs

4.6 Structure property relationship of BR nanocomposites

The above studies reveal that Cloisite 20A and Cloisite 30B show best properties at 3 phr loading. In the present section, structure property relationship of various nanocomposite is established which can explain the reasons to have the above properties.

The structure property relation of matrix (polybutadiene rubber) and nanofillers are discussed with X-Ray Diffraction (XRD), which is used to study the expansion of the nanofillers interlayer distance. XRD patterns of nanocomposites such as BR/Cloisite 20A (3 and 8 phr), BR/Cloisite 30B (3 and 8 phr), BR/CNT (1, 3 and 8 phr) and their raw samples are examined. Also d-spacing values calculated for the same samples and are shown in Table 4.6.

XRD patterns of **BR/ Cloisite 20A** (3 and 8 phr) NCs and its raw filler sample are shown in Figure 4.7. The diffraction peaks of composites are shifted towards low-angle direction; hence the d-spacing values has increased as compared to the raw sample ($\theta \propto 1/\mathrm{d}$). This indicates that effective expansion of the interlayer distance of clay (Cloisite 20A) has occurred within the BR composites. The peak of raw Cloisite 20A at ~3.31° (2θ) has been shifted to below 1.5°. The peak intensites have been decreased also.The d-spacing value of BR/Cloisite 20A (3 phr) nanocomposite has expanded to 20 nm (i.e. about 7.80 nm more from its original 12.20 nm) and for 8 phr it has reached 6.70 nm far from original value, which is 1.10 nm less than the 3 phr sample as shown in Table 4.6. So the above values indicate that the intercalated structure of BR/Cloisite 20A hybrids has been obtained. Degree of intercalation is higher at 3 phr loading. This is the reasion why 3 phr based BR/Cloisite 20A shows better tensile properties than 8 phr filled sample.

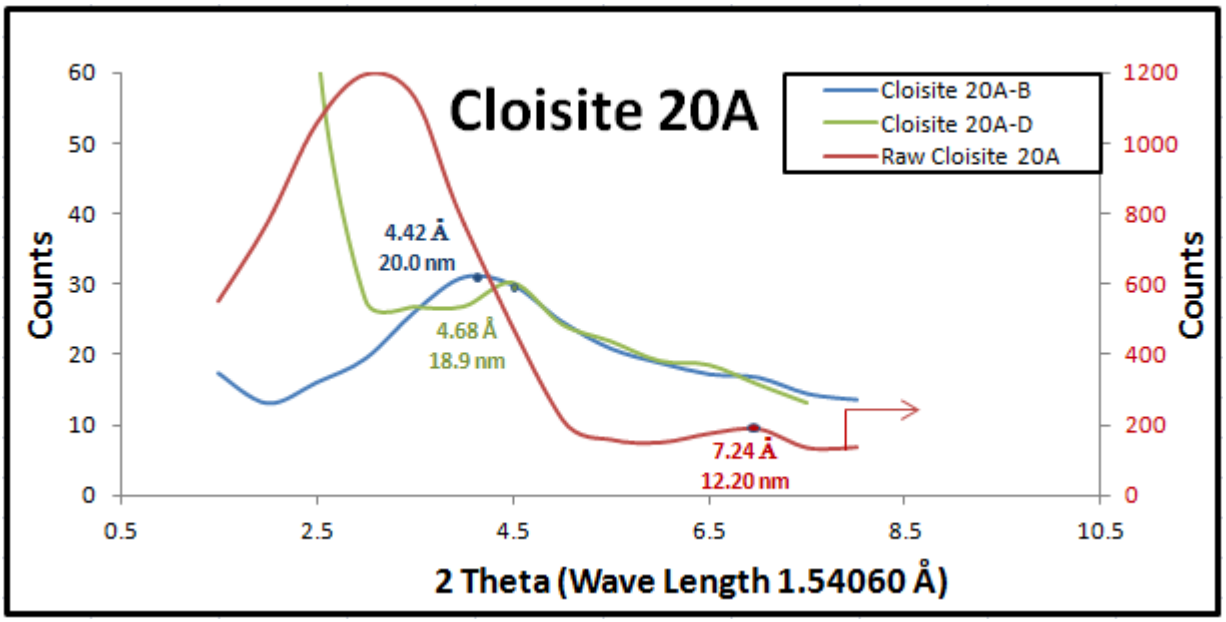

Figure 4.7: XRD patterns of the BR/Cloisite 20A NCs and row Cloisite 20A powder

Table 4.6: 2θ and the corresponding d-spacing values of Cloisite 20A nanocomposites

Sample name	2θ (Å)	d-spacing (nm)
Row Cloisite 20A	7.24	12.20
BR/Cloisite 20A-B	4.42	18.90
BR/Cloisite 20A-D	4.68	20

Similarly XRD patterns of **BR/ Cloisite 30B** (3 and 8 phr) hybrids and its raw filler sample are depicted in Figure 4.8. Also d-spacing values calculated for the same samples and are shown in Table 4.7. The diffraction peaks of composites are shifted towards law-angle direction, which indicates effective expansion of the interlayer distance of clay (Cloisite 30B) within the BR composites. The peak of row Cloisite 30B at ~4.5° (2θ) has been shifted to below 1.5°. The peak intensites have been decreased also. The d-spacing value of BR/Cloisite 30B (3 phr) nanocomposite expands to 19.70 nm (i.e. about 8.23 nm more from its original 11.47 nm) and for 8 phr it reaches 7.23 nm far from original value, but which is 1.0 nm less than that of 3 phr sample. So the above results indicate that BR/Cloisite 30B hybrids have successfully obtained the intercalated or exfoliated structure. Here degree of intercalation in 3 phr filled sample imparts better property improvement than higher filler loading (8 phr).

Table 4.7: 2θ and the corresponding d-spacing values of Cloisite 30B nanocomposites

Sample name	2θ (Å)	d-spacing (nm)
Raw Cloisite30B	9.27	12.20
BR/Cloisite 30B-B	19.70	20
BR/Cloisite 30B-D	18.73	18.90

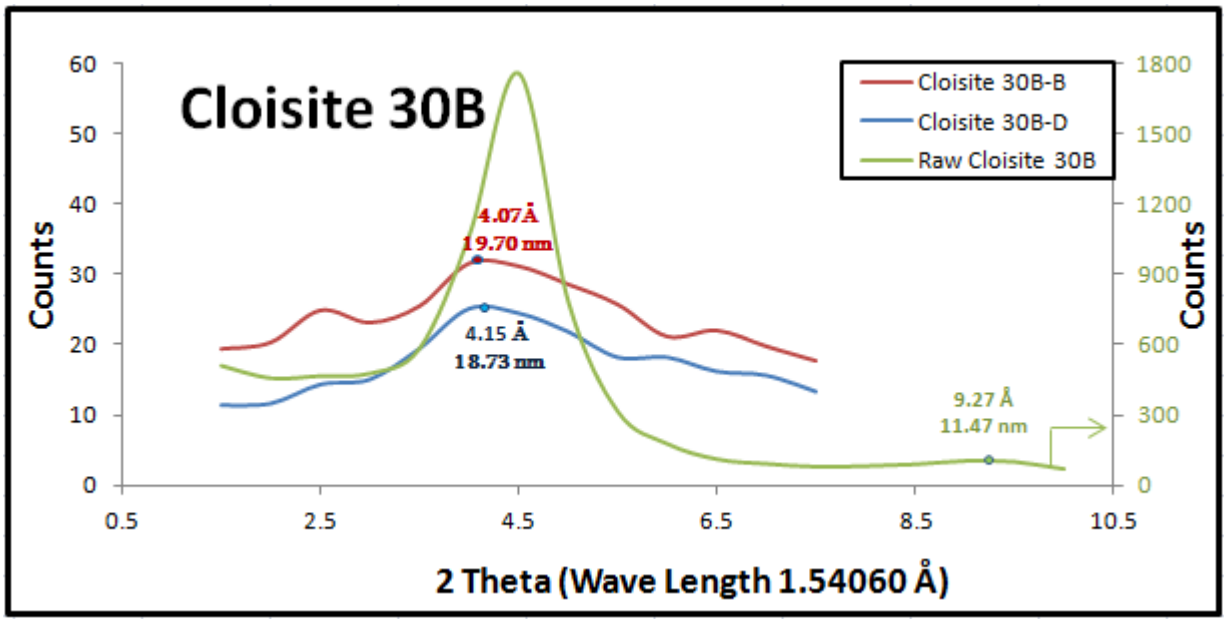

Figure 4.8: XRD patterns of the BR/Cloisite 30B NCs and row Cloisite 30B powder

XRD patterns of **BR/CNT** hybrids and its raw sample are shown in Figure 4.9. The diffraction peaks of composites are shifted towards law-angle direction, which indicates effective expansion of the interlayer distance of CNT within the BR composites. The d-spacing value of BR/CNT NCs (3 and 8 phr) has expanded to 19.6 nm i.e. about 12.12 nm more from its original 7.48 nm.

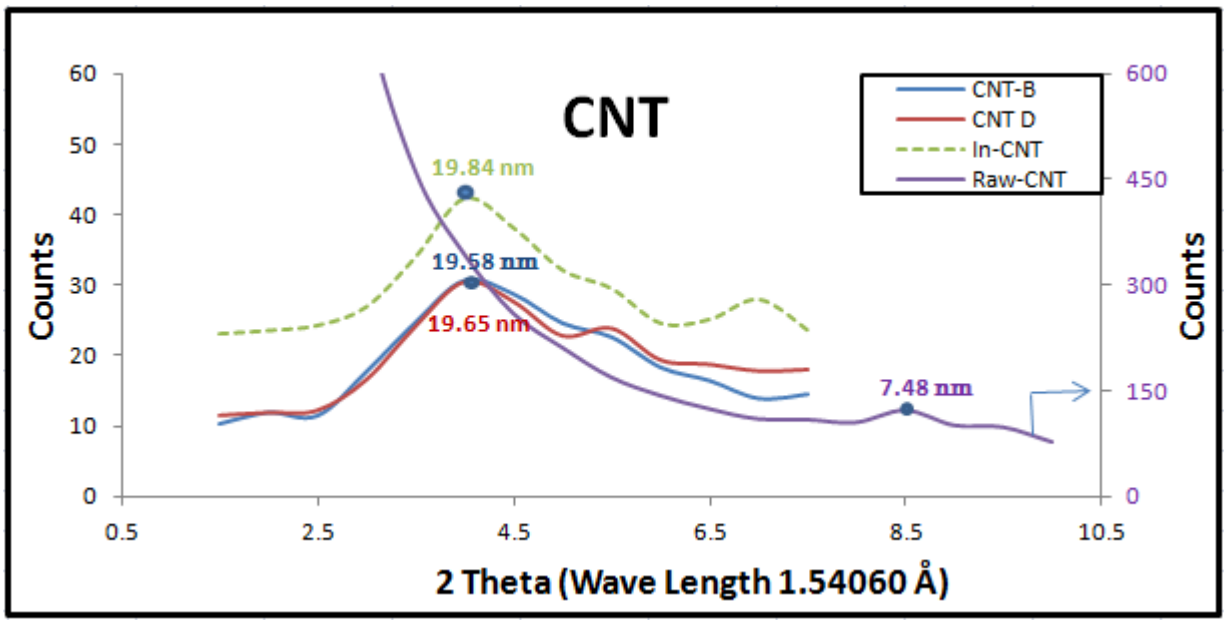

Figure 4.9: XRD patterns of the BR/CNT NCs and row CNT powder

4.7 Comparison of nanocomposites with conventional composites

Different composites are prepared by melt compounding method. Here the composites are classified in two different classes, based on their filler constituents (1) Silica-based composites and (2) Carbon based composites. Reinforcing effect of conventional as well as nanofillers on physico-mechanical properties on gum BR vulcanizates is discussed in this section. The physico-mechanical properties of the BR composites are reported in Table 4.8.

Table 4.8: Physico-mechanical properties of the BR composites

Sample	T.S (MPa)	EB %	300% MOD (MPa)	100% MOD (MPa)	Hardness	Crosslink density X E-05
BR	1.66	302	1.09	0.68	41.0	3.35
BR/ CNT-A	1.86	523	1.08	0.60	50.0	3.72
BR/ CNT-B	2.31	447	1.39	0.74	53.0	4.89
BR/ CNT-C	3.93	432	2.66	1.07	54.0	4.24
BR/ CNT-D	3.33	386	2.86	1.19	54.4	4.31
BR/ CNT-E	2.97	199	2.63	1.29	54.0	6.02
BR/ CB-B	2.04	299	1.38	0.66	43.0	5.58
BR/ CB-C	2.47	367	1.37	0.73	45.0	4.99
BR/ CB-D	2.62	438	1.70	0.76	47.0	4.95
BR/ CB-E	3.59	436	1.41	0.77	48.5	4.08
BR/ Nanosilica-Silane-A	1.71	590	1.01	0.69	51.0	3.56
BR/ Nanosilica-Silane-B	3.72	642	1.80	0.83	55.0	4.22
BR/ Nanosilica-Silane-C	2.36	580	1.22	0.63	53.0	3.57
BR/ Silica-Silane-B	2.11	210	1.68	0.85	45.0	4.26
BR/ Silica-Silane-C	2.04	338	1.13	0.93	47.0	3.71
BR/ Silica-Silane-D	2.07	158	1.10	0.96	44.0	3.60

Here notification –A, -B, -C, -D and –E stands for 1, 3, 5, 8 and 10 wt % of filler composition respectively. A remarkable increase in the physico-mechanical properties of BR/CNT and BR/Nanosilica-Silane hybrids are obtained against conventional filler BR/CB and BR/Silica-Silane.

A continuous increment in the mechanical properties is observed for the **BR/Carbon black (CB)** NCs with increasing filler loading. TS and EB of (10 phr) BR/CB composite are improve by 116% and 44% respectively compared to gum BR vulcanizates. 29% and 13% improvement can be seen in the 100 and 300% modulus respectively compared to BR. The relationship of the filler loading with tensile properties of BR/CB is shown in Figure 4.10. Hardness improves up to 18% than that of BR hybrid. In addition, the crosslink density is also improved. The physico-mechanical properties of BR/CNT NCs are reported in Table 4.8.

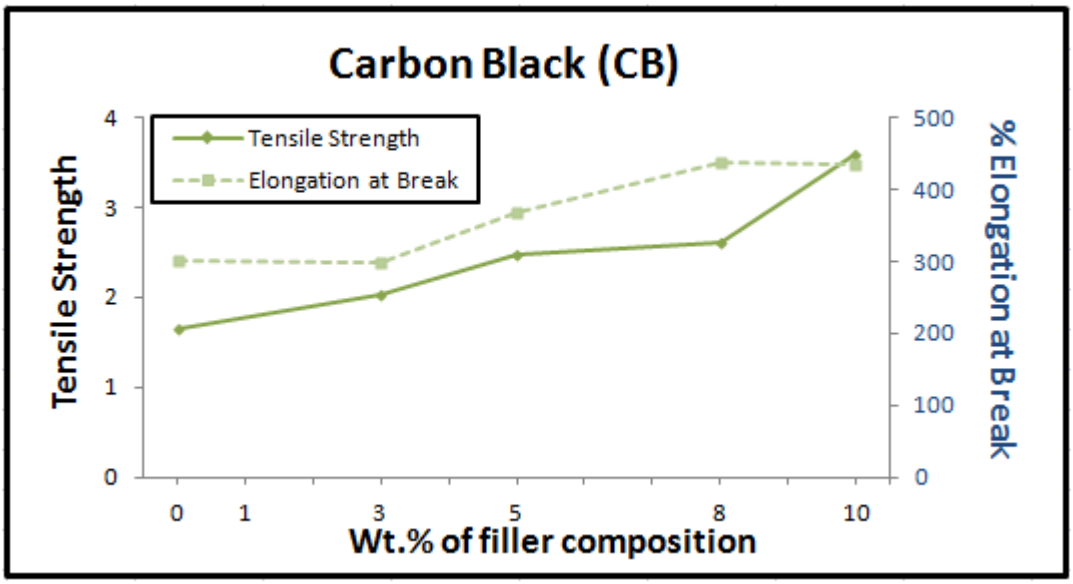

Figure 4.10: Effect of filler loading on tensile properties of BR/CB composites

For the **BR/precipitated silica-silane** NCs, a little influence in the mechanical properties is obtained. The TS of (5 phr) BR/precipitated silica-silane composite is found to be 23% higher as compared to BR. Hardness has improves up to 15% than that of gum BR vulcanizates . The relationship of the filler loading with tensile properties of BR/precipitated silica-silane is shown in Figure 4.11. The physico-mechanical properties of BR/CNT NCs are reported in Table 4.8.

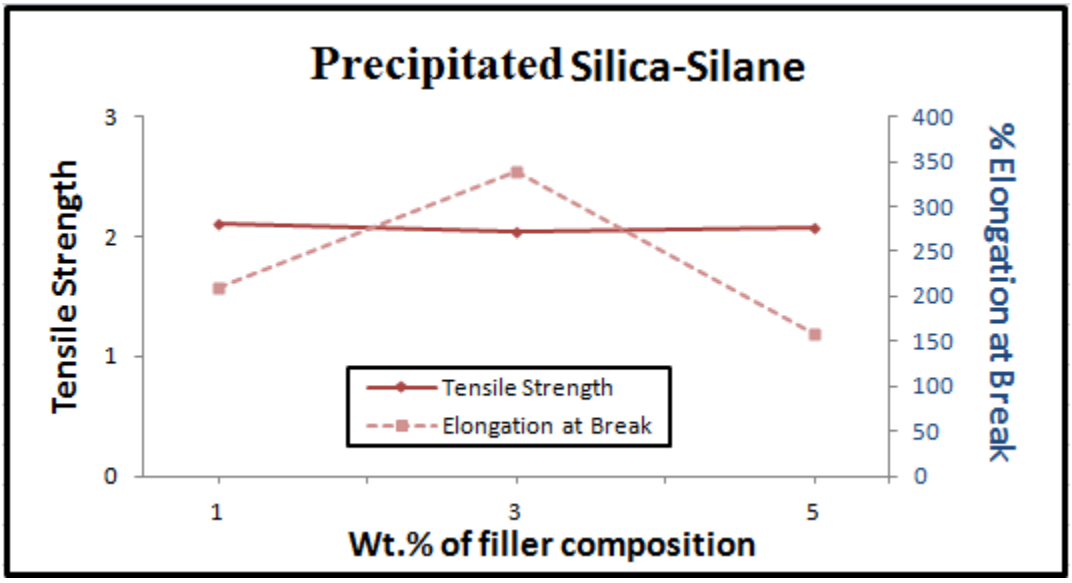

Figure 4.11: Effect of filler loading on tensile properties of BR/precipitated silica-silane composites

The above results show that the BR NCs filled with filler nanosilica possess the highest

physico-mechanical properties followed by CNT against two conventional fillers; carbon black and silica at low filler loading. The smaller particle size provides a larger surface area for the interaction between filler and rubber matrix in the case of nanofillers. The nanofillers CNT and nanosilica have a larger surface area than carbon black and silica, so they exhibit better properties than conventional filler. BR/CNT at 5 phr and BR/Nanosilica-silane at 3 phr possess the highest properties due to intercalated-exfoliated structure of composites and agglomeration of filler in composites at higher filler loading which is also confirmed by X-Ray Diffraction (XRD) results as discussed in section 4.6.

A comparison of TS and EB of BR NCs filled with CNT, CB, Nanosilica and Silica is shown in Figure 4.12. The increment of 59% and 18% respectively is seen in TS and EB of BR/CNT-C hybrid and for 100 and 300% modulus, 20% and 15% improvement respectively is recorded as compared to BR/CB-B composite. In BR/Nanosilica-Silane and BR/Silica-Silane composites also same kind of enhancements has been observed. The TS and EB of BR/Nanosilica-Silane-B composite are 76% and 206% higher respectively compared to BR/Silica-Silane-B. 10% increment is also seen for 300% modulus of BR/Nanosilica-Silane-B hybrid compared to BR/Silica-Silane-B hybrid.

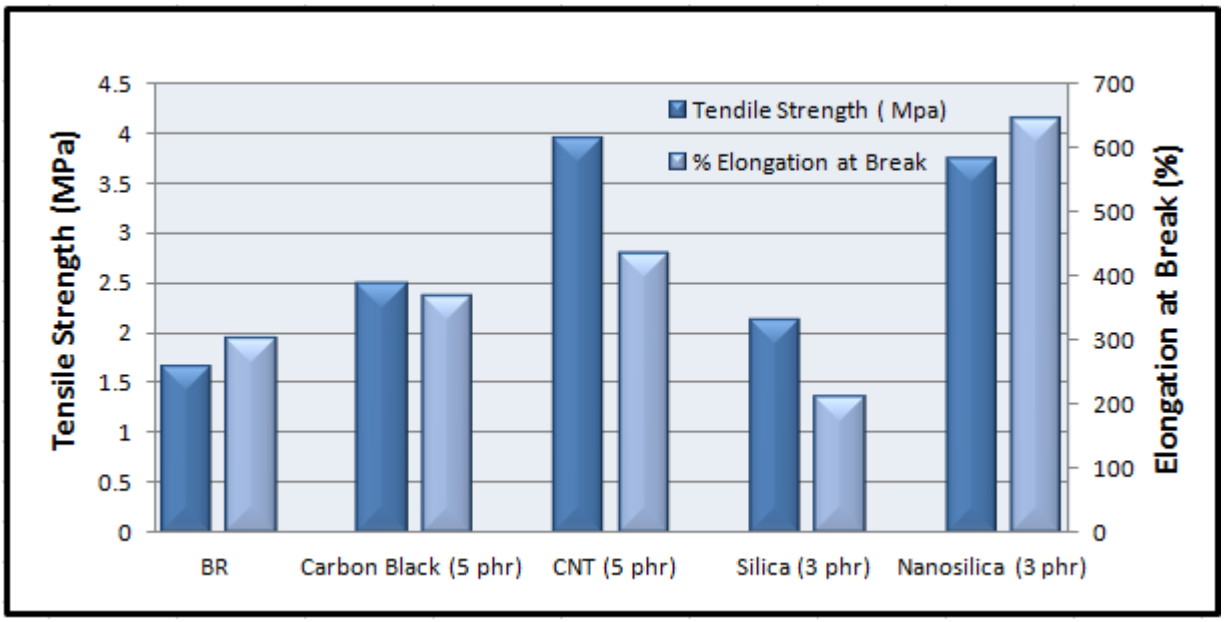

Figure 4.12: Tensile strength and elongation at break of CNT, carbon black, nanosilica and silica filled composites

An improvement of 20% in hardness is observed in both BR nanocomposites (BR/CNT-C and BR/Nanosilica-Silane-B) as compared to conventional composites (BR/CB-C and BR/Silica-Silane-B). Hardness and 300 % modulus of BR composites filled with CNT and CB (at 5 phr), Nanosilica and Silica (3 phr) are compared in Figure 4.13. 300 % modulus of BR/CNT-C improve by 95% as compared to BR/CB-B composite. Though there is a little improvement with nanosilica-silane composite.

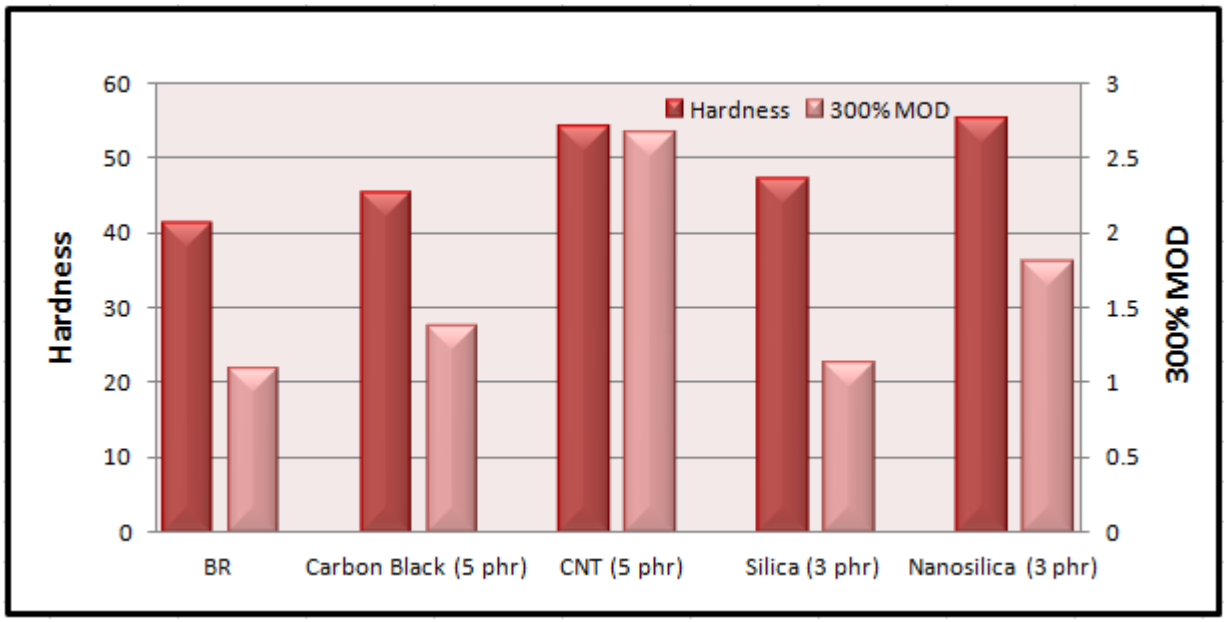

Figure 4.13: Hardness and 300% MOD of CNT, carbon black, nanosilica and silica composites

Physico-mechanical properties of various conventional and nanofillers are discussed in the above sections prepared via *ex situ*/melt blending process. Some good results are observed with CNT, nanosilica and organoclay based BR nanocomposites. A further study using these fillers is done via in situ process with an aim to have better dispersion of nanofillers and to observe their impact on the physico-mechanical properties of BR nanocomposites. It has been discussed comprehensively in the following section.

Literature reports show that BR NCs have been prepared by various routes, but among them the most common problem is weak interaction or poor dispersion of nanofillers in organic compound. As compared to *ex situ* process, *In situ* polymerization method can create strong chemical bonding within the NCs and are expected to produce a more stable and higher quality NCs [43].

4.8 BR nanocomposites via *In situ* polymerization

The monomer 1, 3-Butadiene undergoes stereospecific polymerization to produce high molecular weight cis-1, 4-polybutadiene (>97% cis-1, 4 content) in the presence of soluble catalysts comprising Cobalt Octoate (CoO) and diethylaluminium chloride (Et2AlCl). These polymerization reactions are undertaken in either three necked round bottom flask or Buchi reactor based on the volume of the feed. Nanofillers are incorporated within the polymerization reaction. It is proposed to have better dispersion withun gum BR vulcanizates and to form more stable and higher quality nanocomposites. Further comppounding of these materials is done by melt-mixing.

For polymerization reaction various fillers are incorporated separately in order to check for the progress of the reaction. These fillers are CNT, nanosilica, closite 20A, closite 30B and

pangel B20, among these successful polymerization reactions occur with CNT and nanaosilica only.

The physico-mechanical properties of the BR nanocomposites (1phr) produced by *In situ* polymerization method are reported in Table 4.9. Significant increments in the mechanical properties of nanocomposites are shown in Figure 4.14.

Table 4.9: Mechanical properties of the BR NCs produced by *In situ* polymerization

Sample (1 phr)	T.S (MPa)	EB %	300% MOD (MPa)	100% MOD (MPa)	Hardness	Crosslink density X E-05	Intrinsic Viscosity (η)	Viscosity avg. molecular weight (Mv)
In-BR	1.27	557	0.69	0.54	42	1.62	2.20	2,09,505
In-CNT	1.33	570	0.74	0.61	52.5	1.71	3.02	3,24,564
In-nanosilica	2.18	670	1.00	0.67	48.5	1.90	3.14	3,41,779

The above results show that BR/In-nanosilica and BR/In-CNT NCs possess better mechanical properties at only 1 phr filler loading against the In-BR gum vulcanizates. For BR/In-nanosilica composite, TS and EB has improve by 72% and 20% respectively and for 100 and 300% modulus, 45% and 24% respectively improvement is recorded as compared to In-BR. Crosslink density, intrinsic viscosity and molecular weight of BR/In-nanosilica and BR/In-CNT nanocomposite has also improve significantly compared to In-BR. Figure 4.9 shows as expected, in situ polymerization has shown a d-spacing value 0.25 nm higher than *ex situ* method, for only 1 phr BR/CNT hybrid. The results and data indicate that the problems of weak interaction or poor dispersion of nanofillers in organic compound has been overcome by the *in situ* polymerization method.

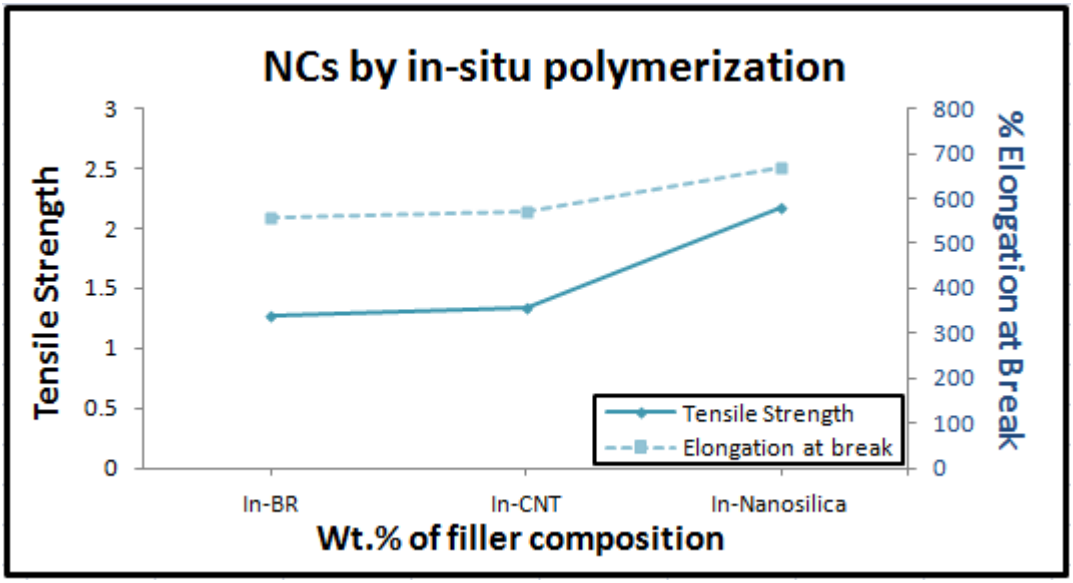

Figure 4.14: TS and EB of NCs prepared by *in situ* polymerization

4.9 Effect of nanofillers on swelling behaviour

Addition of nanofillers increases the volume fraction of the rubber, causing a decrease in overall solvent swelling. The swelling always decreases with increasing filler loading [32]. The nanofillers like CNT and nanosilica are better exfoliated and having better intercalation with the rubber shows lower swellimg compared to that of unmodified BR hybrid sample as shown in Figure 4.15. The equilibrium solvent uptake is minimum in In-nanosilica followed by In-CNT sample.

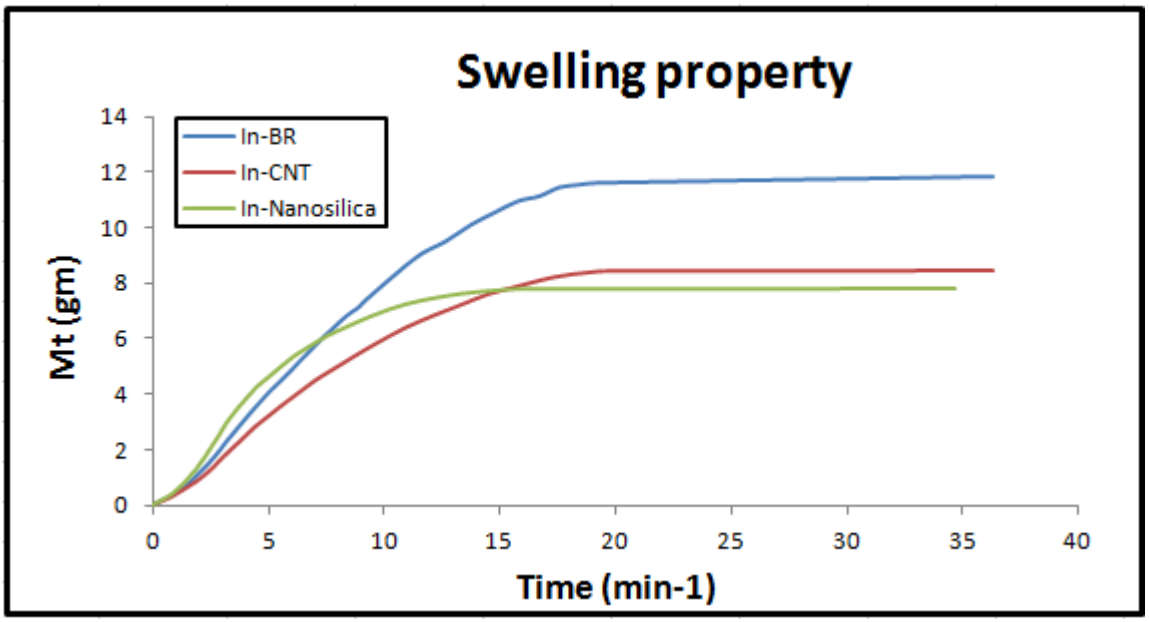

Figure 4.15: Mass up taken (Mt) versus Time of BR/NCs produced by *In situ* polymerization

In order to understand, the effect of filler loading on swelling behaviour, BR/CNT NCs with 1, 3, 5 and 8 phr are tested. The swelling values decrease with increasing in the CNT loading as expected. The swelling behaviour of BR/CNT NCs are shown in Figure 4.16. Also decrement in equilibrium swelling of BR/CNT NCs observed with increase CNT loading as shown in Figure 4.17.

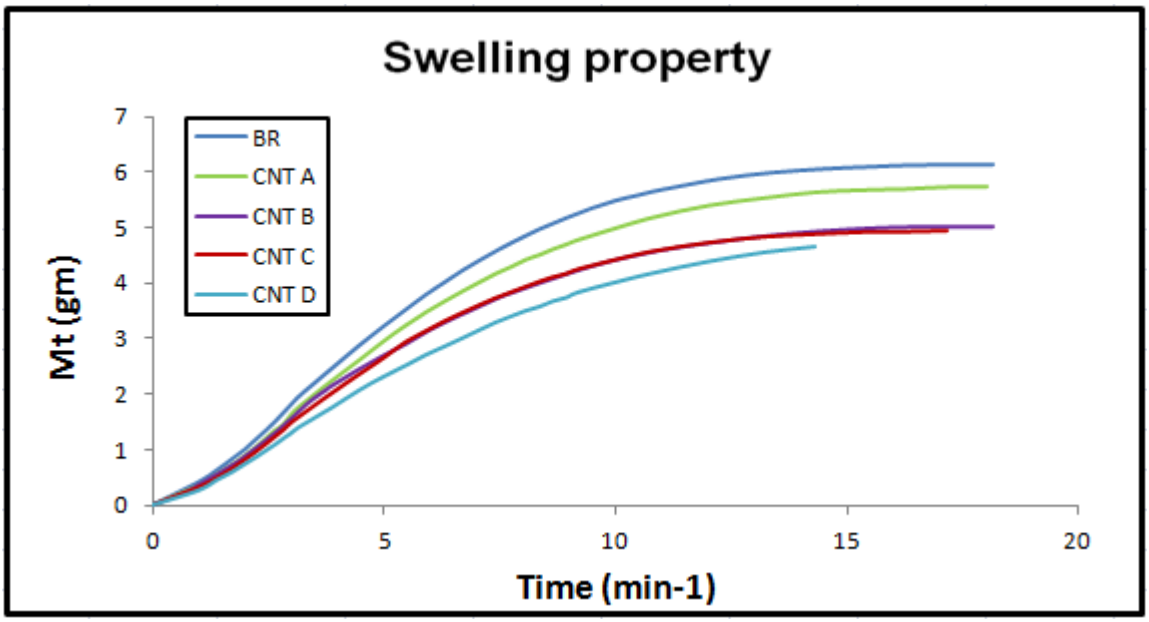

Figure 4.16: Mass up taken (Mt) versus Time of BR/CNT Ncs

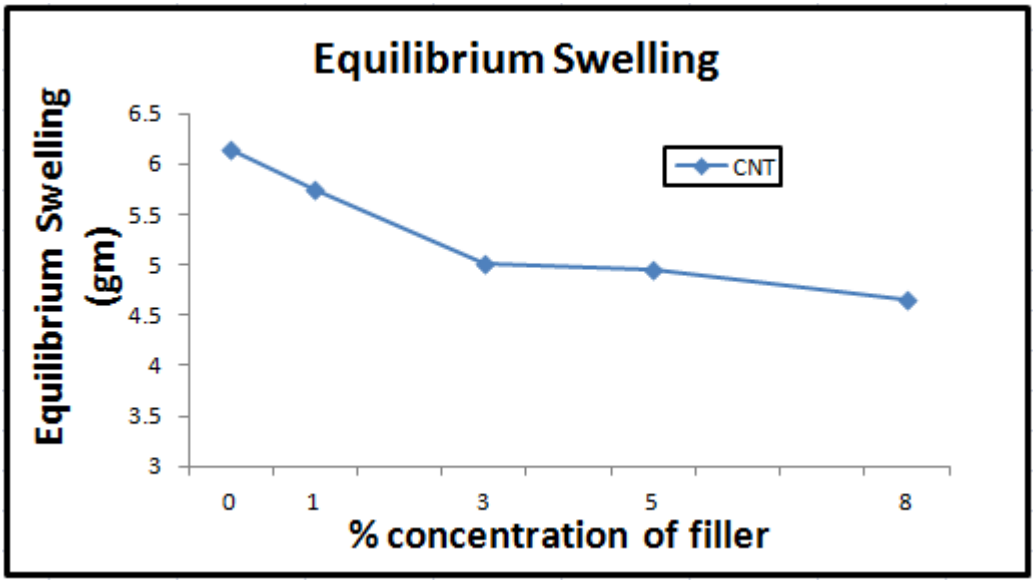

Figure 4.17: Effect of % concentration of filler loading on equilibrium swelling

4.10 Thermal properties of BR nanocomposites

The thermal decomposition behaviour of BR NCs is assessed by thermogravimetric analysis (TGA) and derivative thermogravimetric analysis (DTG) curves which are shown in Figure 4.18 and 4.19.

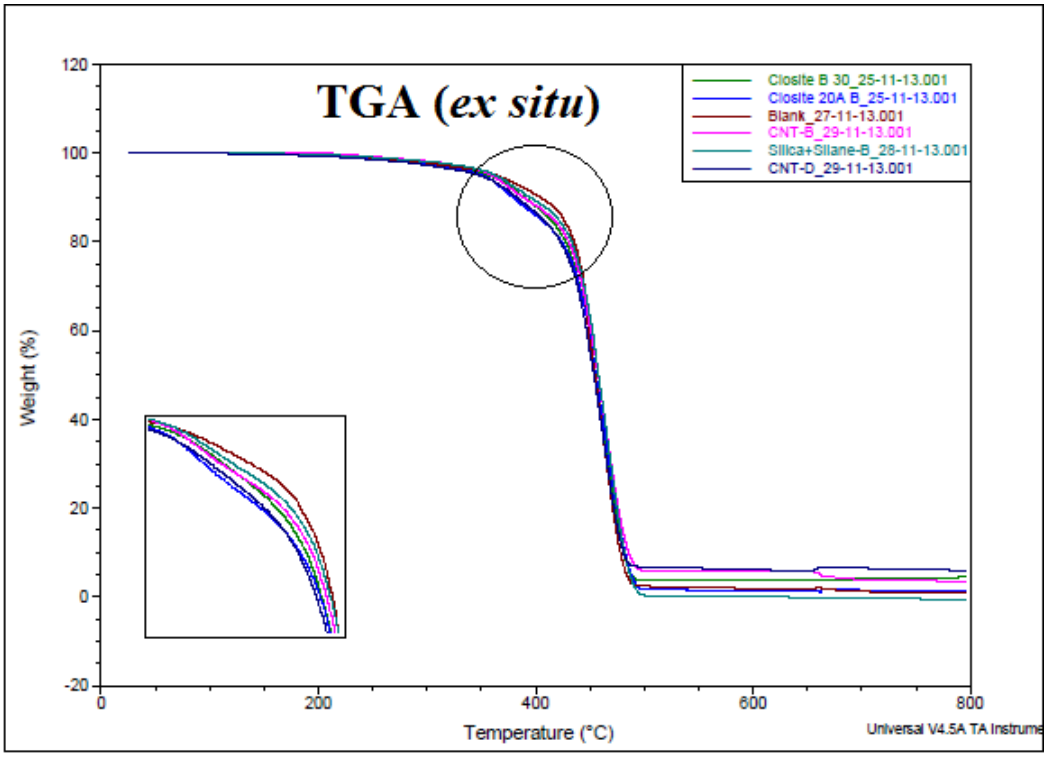

Figure 4.18: TGA curves of BR nanocomposites

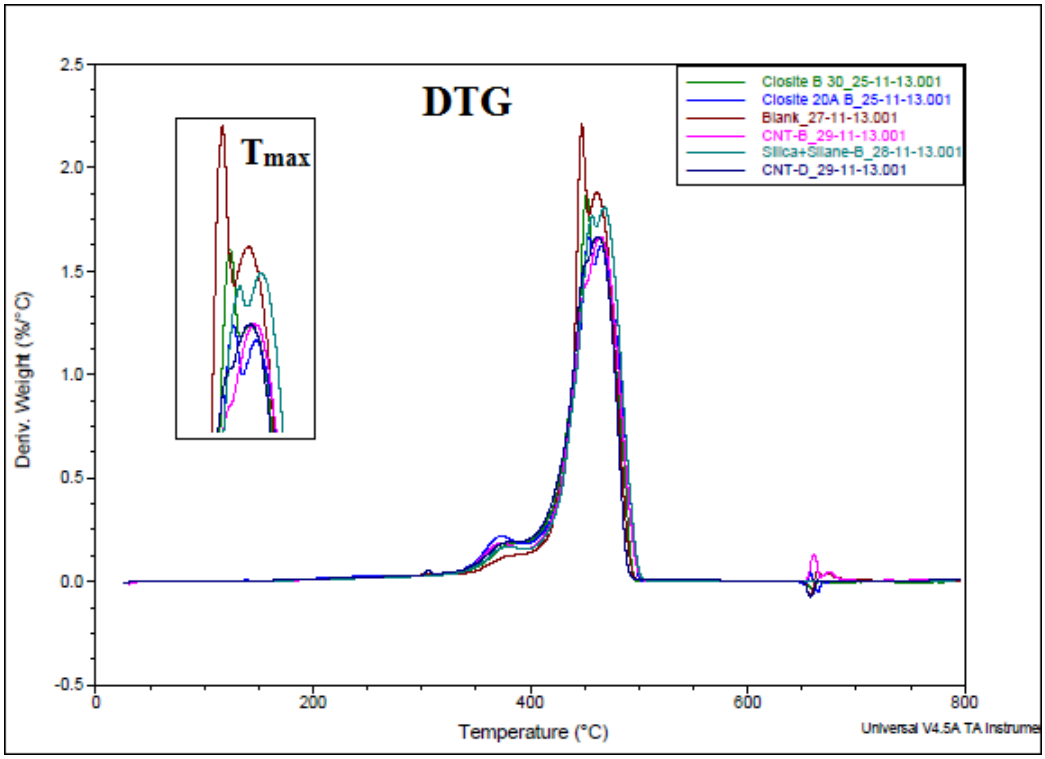

Figure 4.19: DTG curves of BR nanocomposites

The results are reported in Table 4.10 in terms of T_{max} (Temperature corresponding to the maximum value in the derivative thermogram) and T_{onset} (Temperature corresponding to 5% degradation). It shows that T_{max} increases and T_{onset} decreases with the incorporation of nanofillers.

The T_{max} values for BR/CNT -B and BR/CNT -D NCs are increase by 16°C and 13°C respectively as compared to BR. For BR/nanosilica-silane-B composite, 7°C improvement is recorded. For silicates BR/Cloisite 20A -B and BR/Cloisite30B -B composite, 1°C and 4°C respectively improvement is recorded as compared to BR hybrid. The reason behind is the nanoscale dispersion of CNT and Nanosilica. The natural thermal stability of nanofillers has been achieved completely, hence it proves that the NCs which having a strong interaction with the matrix also have a better thermal stability. These analyses suggest that BR has the best thermal stability with nanofillers like CNTs and nanosilica.

Table 4.10: First derivative temperatures of BR nanocomposites

Weight Loss Temperature	BR nanocomposites					
	BR	Cloisite 30B-B	Cloisite 20A-B	CNT-B	CNT-D	nanosilica-B
T_{onset}	375	369	355	362	357	364
T_{max}	450	451	454	466	463	457

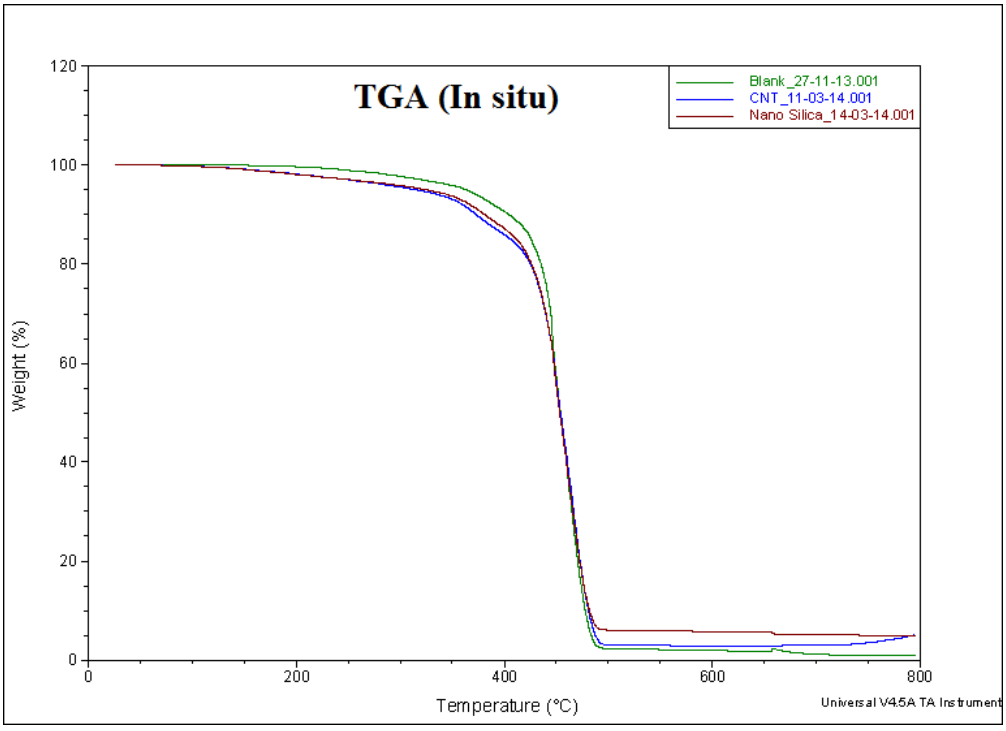

Figure 4.20: TGA curves of BR nanocomposites prepared via *in situ* process

The thermal decomposition behaviour of BR NCs prepared via *in situ* process is assessed

by TGA-DTG curves which are shown in Figure 4.20 and 4.21. The results are reported in Table 4.11 in terms of $T_{max}$and T_{onset}. It shows that T_{max} increases and T_{onset} decreases with the incorporation of nanofillers. The T_{max} value for BR/in-CNT nanocomposite increase by 9°C and for BR/in-nanosilica nanocomposite increase by 7°C compared to in-BR.

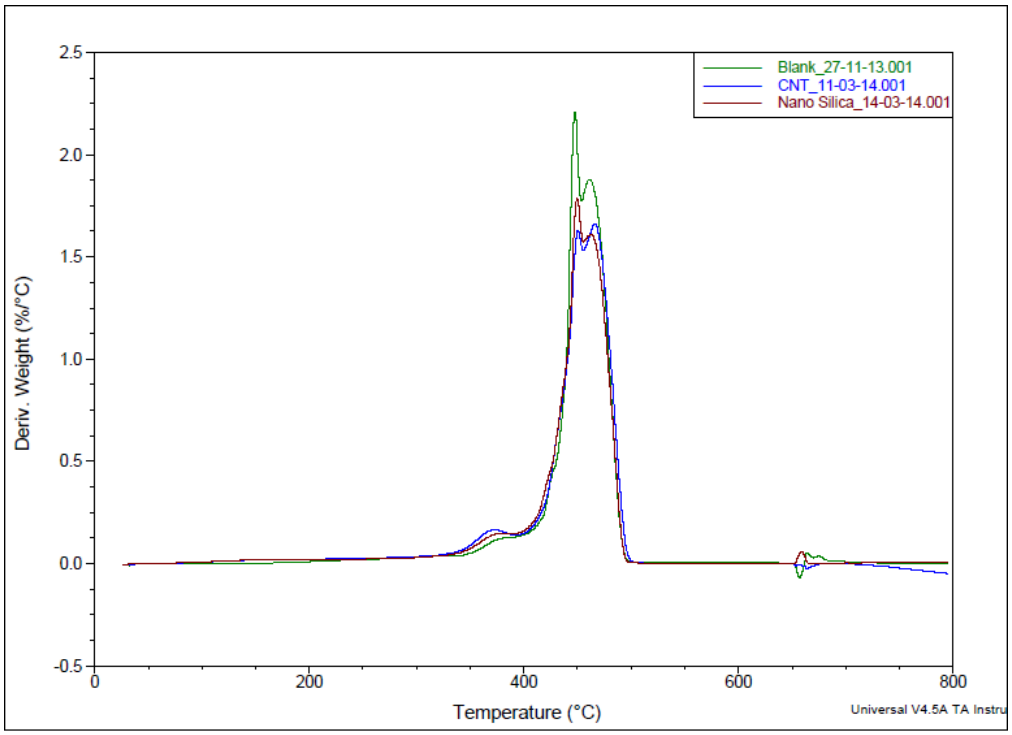

Figure 4.21: DTG curves of BR nanocomposites prepared via *in situ* process

Table 4.11: First derivative temperatures of BR nanocomposites prepared via *in situ* process

Weight Loss Temperature	BR nanocomposites		
	In-BR	In-CNT	In-nanosilica
T_{onset}	375	345	347
T_{max}	450	459	457

Chapter 5

Conclusions

The present investigation is initiated with a primary objective of preparing BR based nanocomposites using various kinds of nanofillers via both *in situ* and *ex situ* process. Although *ex situ* prepared nanocomposites of elastomers is not a new area of concern, but the in situ prepared nanocomposites are scarcely available in the literature; in the true sense, BR nanocomposites prepared via *in situ* method have not been explored in detail before the present study. Moreever to prepare *in situ* BR in a process similar to commercial one in a real challenge.

The BR based nanocomposites are successfully prepared by both *in situ* and *ex situ* methods. Effect of nanofiller loading is investigated on the properties of prepared nanocomposites by *ex situ* melt blending. The nanocomposites were also compared with conventional composites. The *in situ* nanocomposites where tried to be synthesised with the filler, which showed best overall properties in *in situ* nanocomposites. Furthermore, the reaction condition parameters are well optimized in the in situ process. The intricate analysis and subsequent discussion on the experimental finding leads to the following conclusions:

1. The characterization of nanofillers is carried out by using powder X-ray diffraction (XRD), and BET-surface area measurements. Surface area of all nanofillers are higher than the conventional fillers.

2. Nanofillers import tremendous enhancement in physico-mechanical properties. For example, in the *ex situ* process, the BR nanocomposites containing 3 phr loaded Cloisite 20A showed 245% and 220% improvement in tensile strength and %EB respectively, also 41% and 50% improvement in hardness and density respectively as compared to the matrix devoid of nanomaterial.

3. Among different groups of nanofillers, e.g., nanoclay, hydrotalcite, nanosilica and CNT, Cloisite 20A, Cloisite 30B, nanosilica-silane and CNT showed best properties.

4. Best properties were observed in the range of 3-5 phr which is far lower than the conventional dosing of conventional fillers.

5. Physico-mechanical properties of nanocomposites decrease with increasing filler loading.

6. XRD of nanocomposites showed intercalated-exfoliated structure at low filler loading through the degree of intercalation decreases at higher filler loadign. This is why properties show a declining trend at higher filler loading.

7. Nanocomposites show better properties at lower filler loading than the conventional composites with carbon black and silica. Thus, much lighter rubber product can be produced by nanocomposite route.

8. Dispersion problem of nanofillers can be overcome by developing *in situ* nanocomposites.

9. *In situ* nanosilica based composites show better physico-mechanical properties than *ex situ* one.

10. The thermal and swelling properties are also improved remarkably in the nanocomposites compared to gum BR vulcanizate in corroboration with physico-mechanical properties.

Chapter 6

Scope for future work

Due to time constraint, some studies could not be covered in the present thesis, which can be taken further.

1. To synthesize *in situ* nanocomposites with more number of nanofillers.
2. To synthesize *in situ* nanocomposites at different filler loading.
3. To study the physico-mechanical and thermal properties in detail.
4. To study the detailed morphology of the nanocomposites.

Bibliography

[1] I. Hamid and G. Kumar; Molecular Characterization of Composite Interfaces, Eds. Plenum, New York, (1985)

[2] E.P. Plueddemann; Interfaces in Polimar Matrix Composites, Academic Press, San Diego, (1994)

[3] V.Jha; Carbon Black Filler Reinforcement of Elastomers, Department of Materials, Queenmary, London, (2008)

[4] S.D. Sadhu, M. Maiti and A.K. Bhowmick; Elastomer–Clay Nanocomposites, Current Topics in Elastomers Research, CRC Press, United States, (2008)

[5] M. Alexandre and P. Dubois; Journal of Material Science Engineering, vol. 28, p. 1-63, (2000)

[6] N. Thuadaij, A. Nuntiya and M. Chiang Journal of Science; vol. 35, p. 206-211, (2008)

[7] C. V. Clemency and E. Bunesberg; Journal of Clays and Clay Miner, vol. 21, p. 213–217, (1973)

[8] A.P. Kumar, D. Depan, N.S. Tomer and R.P. Singh; Journal of Polymer Science, vol. 34, p. 479-515, (2009)

[9] J.K. Kocsis and C.M. Wu; Journal of Polymer Engineering Science, vol. 44, p. 1083, (2004)

[10] U. Sebenik, A. Zupancic-Valant and M. Krajnc; Polymer Engineering and Science, vol. 46, p. 1649-1659, (2006)

[11] S. Mishra, S.H. Sonawane, N. Badgujar, K. Gurav and D. Patil; Journal of Applied Science, Vol. 96, p. 6-9, (2005)

[12] X. Qian, M. Liao and W. Zhang; Journal of Polymer International, vol. 56, p. 399-408, (2007)

[13] M. Liao, W. Shan, J. Zhu, Y. Li and H. Xu; Journal of polymer Science: Part B: Polymer Physics, vol. 43, p. 1344-1353, (2005)

[14] Z. Gu, G. Song, W. Liu, B. Wang and J. Li; Journal of Applied Clay Science, vol.45, p. 50–53, (2009)

[15] D.R. Paul and T.M. Robeson; journal of Polymer, vol. 49, p. 3187-3204, (2008)

[16] S.Wang, Y. Zhang, Z. Peng and Y. Zhang; Journal of Applied Science, vol. 98, p. 227-237, (2005)

[17] A. Das, K.W. Stockelhuber, R. Jurk, M. Saphiannikova, H. Lorenz and M. Kluppel; Journal of Polymer,vol. 49, p. 5276-5283, (2008)

[18] A. Das, K.W. Stockelhuber, R. Jurk, D. Jehnichen and G. Heinrich; Journal of Applied Clay Science, vol. 51, p. 117–125, (2011)

[19] Z. Gu, L. Gao, G. Song, W. Liu, P. Li and C. Shan; Journal of Applied Clay Science, vol. 50, p. 43–47, (2010)

[20] G. Leone, A. Boglia, F. Bertini, M. Cantti and G. Ricci; Journal of polymer Science: Part A: Polymer Chemistry, vol. 48, p. 4473-4483, (2010)

[21] P.L. Teh, Z.A. Mohd Ishak, A.S. Hashim, J. Karger-Kocsis and U.S. Ishiaku; Journal of Polymer Science, vol. 94, p. 2438-2445, (2004)

[22] S. Wang, Y. Hu, Q. ZhongKai, Z. Wang, Z. Chan and W. Fan; Journal of Materials letters, vol. 57, p. 2675-2678, (2003)

[23] M.Z. Rong, M.Q. Zhang and W.H. Ruan; Journal of Materials Science and Technology, vol. 22, p. 787–796, (2006).

[24] S.D. Sadhu and A.K Bhowmick; Jounal of Polymer Science, Part B: Polymer physics, vol. 42, p. 1573, (2004)

[25] A. Lagashetty and A. Venkataraman; Journal of Optoelectronics and Advanced Materials – Rapid Communications, vol. 4, p. 1520 – 1525, (2010)

[26] S.S. Ray and M. Okamoto; Journal of Progress in Polymer Science, vol. 28, p. 1539, (2003)

[27] M. Kim and G. Kim; Journal of Applied Science, vol. 129, p. 3512–3517, (2013).

[28] C. Wan, W. Dong, Y. Zhang and Y. Zhang; Journal of Applied Science, vol. 107, p. 650-657, (2008)

[29] K.G. Gatos, L. Szazdi, B. Pukanszky and K.Karger; Journal of Macromolecule Rapid Communication, vol. 26, p. 915, (2005)

[30] S. Varghese; Journal of Polymer, vol. 44, p. 3977, (2003)

[31] S.H. Wang, Y. Zhang; W.T. Ren, Y.X. Zhang and H. F. Lin; Journal of Polymer Test vol. 24, p. 766, (2005)

[32] S. H. Wang, Y. Zhang, Z.L. Peng and Y.X. Zhang; Journal of Applied Polymer Science, vol. 99, p. 2005, (2006)

[33] S. Sandhu and A.K. Bhowmick; Journal of polymer science: part B: Polymer Physics, vol. 43, p. 1854-1864, (2005)

[34] H. Chen, H. Xiong, Y. Gao and H. Li, Journal of applied polymer science; vol. 116, p. 1272-1277, (2010)

[35] A. Das, K.W. Stockelhuber, R. Jurk, M. Saphiannikova, J. Fritzsche, H. Lorenz, M. Kluppel and G. Heinrich; Journal of Polymer, vol. 49, p. 5276–5283, (2008)

[36] A.A. Kovalchuk, A.N. Shchegolikhin, V.G. Shevchenko, P.M. Nedorezova, A.N. Klyamkina and A.M. Aladyshev; Journal of Macromolecules, vol. 41, p. 3149–56, (2008)

[37] H. Lorenz, J. Fritzsche, A. Das, K.W. Stockelhuber, R. Jurk and G. Heinrich; Journal of Compos Science Technology, vol. 69, p. 2135–43, (2009)

[38] A. Das, K.W. Stockelhuber, R. Jurk, J. Fritzsche, M. Kluppel, G. Heinrich; Journal of Carbon, vol. 47, p. 3313–3321, (2009)

[39] G. Mathew, J.M. Rhee, M.H. Lee and C. Nah; Journal of Advanced Technology, vol. 15, p. 400-408, (2004)

[40] N. Suzuki, M. Ito and F. Yatsuyanag; Journal of Polymer, vol. 46, p. 193-201, (2005)

[41] S.S. Choi, B.H. Park and M. Song; Journal of Polymer Advanced Technology, vol. 15, p. 122-127, (2004)

[42] S.J. Park, S.Y. Jin and S. Kaang; Journal of Polymer Science : Part A, vol. 398, p. 137-141, (2005)

[43] F. Pompeo and D.E. Resasco; Journsl of Nano Letters, vol. 2, p. 369-373, (2002).

[44] K.J. Arun, P.J. Joseph Fransis and R. Joseph; Journal of Optoelectronics and Advanced Material – Rapid Communication, vol. 4, p. 1520 – 1525, (2010)

[45] X. Zhang and L.C. Simon; Journal of Macromolecule Material Engineering vol. 290, p. 573–583, (2005)

[46] Z. Guo, T. Pereira, O Choi, Y Wang and H.T. Hahn; Journal of Material Chemistry vol. 16, p. 2800–2808, (2006)

[47] G.M. Lee, J.W. Yoo and K.B.Lee; Journal of Chemical Engineering Polymer of Japan, vol. 47, p. 159-164, (2014)

[48] T. Fukuda, S. Fujji, Y. Nakamura and M. Sasaki; Journal of Applied Polymer, Science, vol. 130, p. 322-329, (2013)

[49] D.P. Uskokovic, S.K. Milonjic and D.I. Rakovic; Journal of Materials Science Forum, vol. 555, p. 479-484, (2007)

[50] S.Y. Yong, L. Liu, Z.X. Jia, W.W. Fu, D.M. Jia and M.F. Luo; Journal of EXPRESS Polymer Letters, Vol. 8, p. 425-435, (2014)

[51] X. Liu and S. Zhao; Journal of Applied Polymer Science, vol. 108, p. 3038-3045, (2008)

[52] M. Maiti and A.K. Bhowmick; Journal of Applied Polymer Science, vol. 105, p. 435-445, (2007)

[53] J.L. Wilson, P. Poddar, N.A. Frey, H. Srikanth, K. Mohomed, and J.P. Harmon; Journal of Applied Physics, vol.95, p. 1439–1443, (2004)

[54] B.G. Soares, K. dahmouche, V.D. Lima, A.A. Silva and P.C. Caplan; Journal of Colloidal and Interface, vol. 358, p. 338-346, (2011)

[55] V.K. Upadhyay and S. Sivaram; Indian journal of Technology, vol. 29, p. 579-583, (1987)

[56] N. Pires, A. Ferreira, C. Lira, P. Coutinho, L. Nicolini, B. Soares and F. Countinho; Journal of applied Polymer Science, vol. 99, p. 88-99, (2006)

[57] L. Reich and S.S. Stivala; Journal of Polymer Science: Part A, Vol. 1, p. 203-216, (1963)

[58] G. Natta and L. Porri; Polymer Chemistry of Synthetic Elastomer, part-2, edited by J.P. Kennedy and E. Tornqvirst, John Wiley and Sons, New York (1967)

[59] V.K. Upadhyay and S. Sivaram; Indian journal of Technology, vol. 25, p. 667-673 (1987)

[60] A.Singh, S. Modi, N. Subrahmanyam, P. Munshi, V. K. Upadhyay, R.V. Jasra and M. Maiti; Journal of Industrial and Engineering Chemistry Research, vol. 49(20), p. 9648-9654 (2010)

[61] V.K. Srivastav, M. Maiti and R.V. Jasra; Journal of European Polymer, vol. 47(12), p. 2342-2350 (2011)

[62] A. Chavda, S. Nandula, R.V. Jasra and M. Maiti; Journal of Industrial and Engineering Chemistry Research, vol. 51(34), p. 11066-11071 (2012)

Appendices

Appendix 1

XRD Graphs:

Wavelength (λ) = 1.5406 Å , Scanning range (2θ) = 1.5° to 90°

a) Raw Cloisite 20A powder

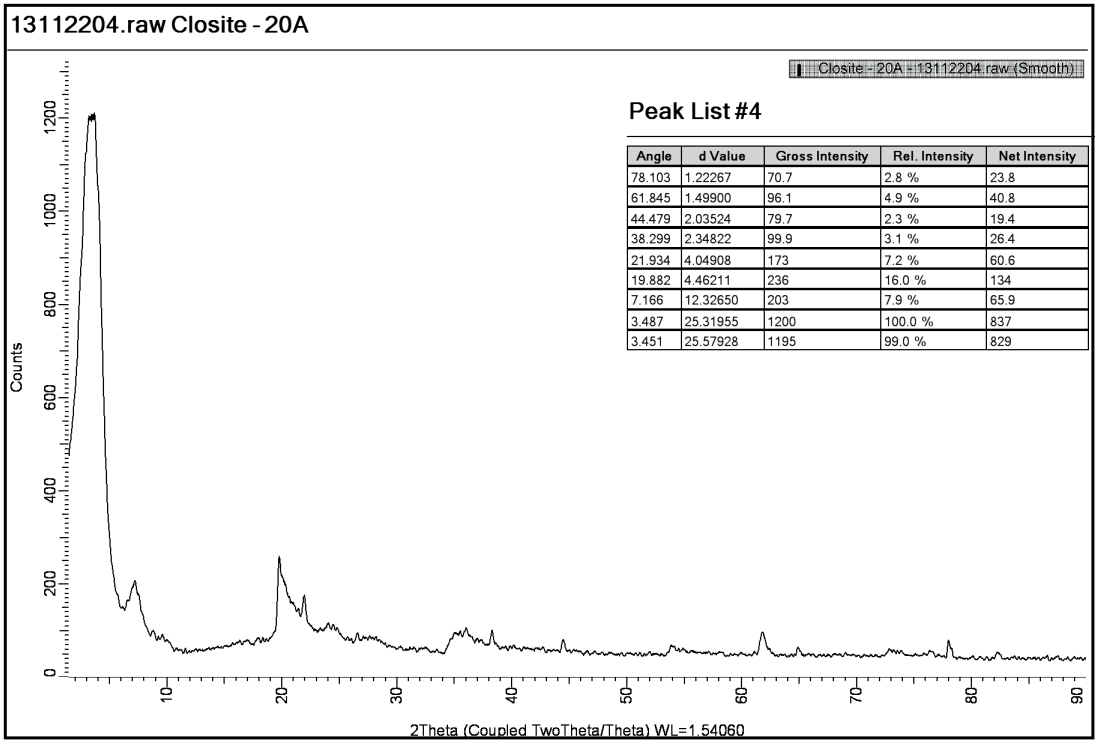

Peak List #4

Angle	d Value	Gross Intensity	Rel. Intensity	Net Intensity
78.103	1.22267	70.7	2.8 %	23.8
61.845	1.49900	96.1	4.9 %	40.8
44.479	2.03524	79.7	2.3 %	19.4
38.299	2.34822	99.9	3.1 %	26.4
21.934	4.04908	173	7.2 %	60.6
19.882	4.46211	236	16.0 %	134
7.166	12.32650	203	7.9 %	65.9
3.487	25.31955	1200	100.0 %	837
3.451	25.57928	1195	99.0 %	829

b) Cloisite 20A -B

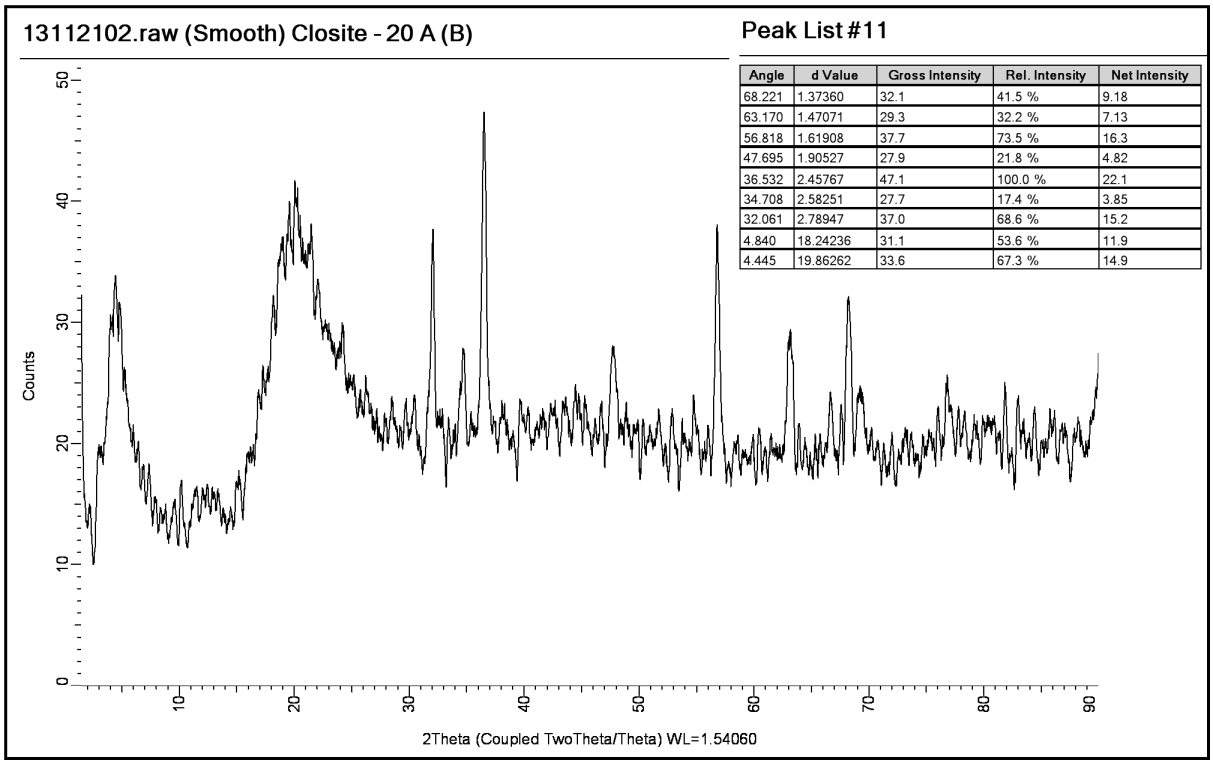

c) Cloisite 20A-D

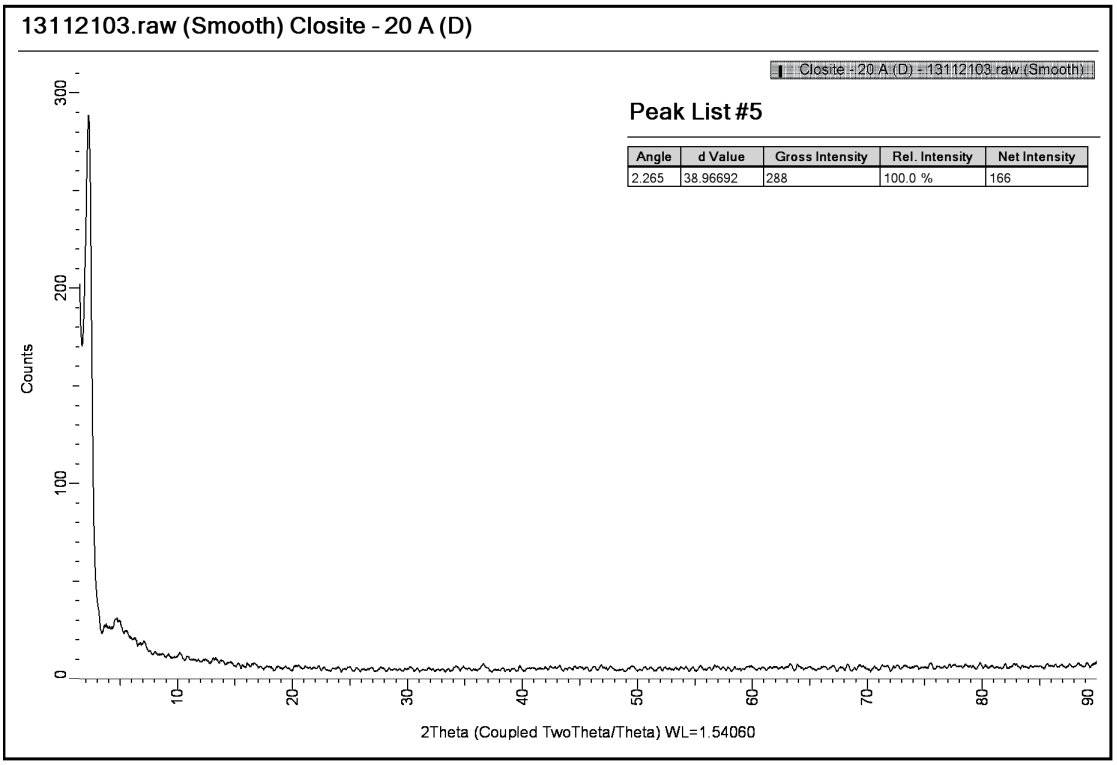

d) Raw Cloisite 30B powder

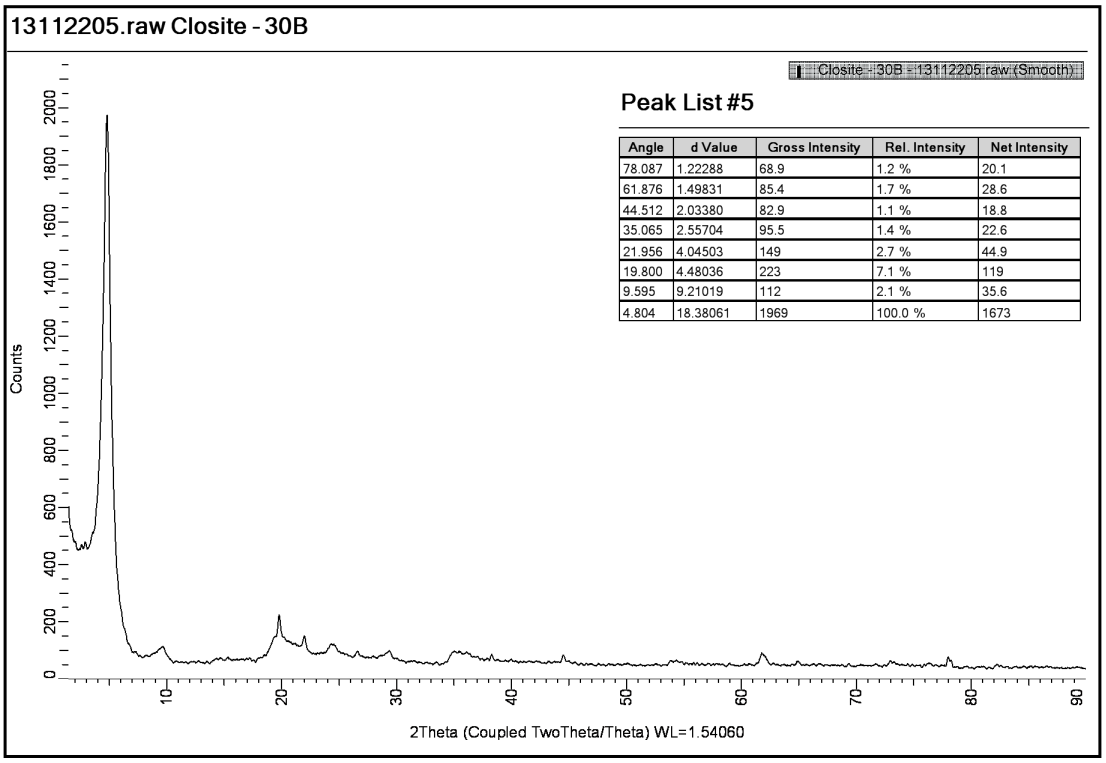

Peak List #5

Angle	d Value	Gross Intensity	Rel. Intensity	Net Intensity
78.087	1.22288	68.9	1.2 %	20.1
61.876	1.49831	85.4	1.7 %	28.6
44.512	2.03380	82.9	1.1 %	18.8
35.065	2.55704	95.5	1.4 %	22.6
21.956	4.04503	149	2.7 %	44.9
19.800	4.48036	223	7.1 %	119
9.595	9.21019	112	2.1 %	35.6
4.804	18.38061	1969	100.0 %	1673

e) Cloisite 30B-B

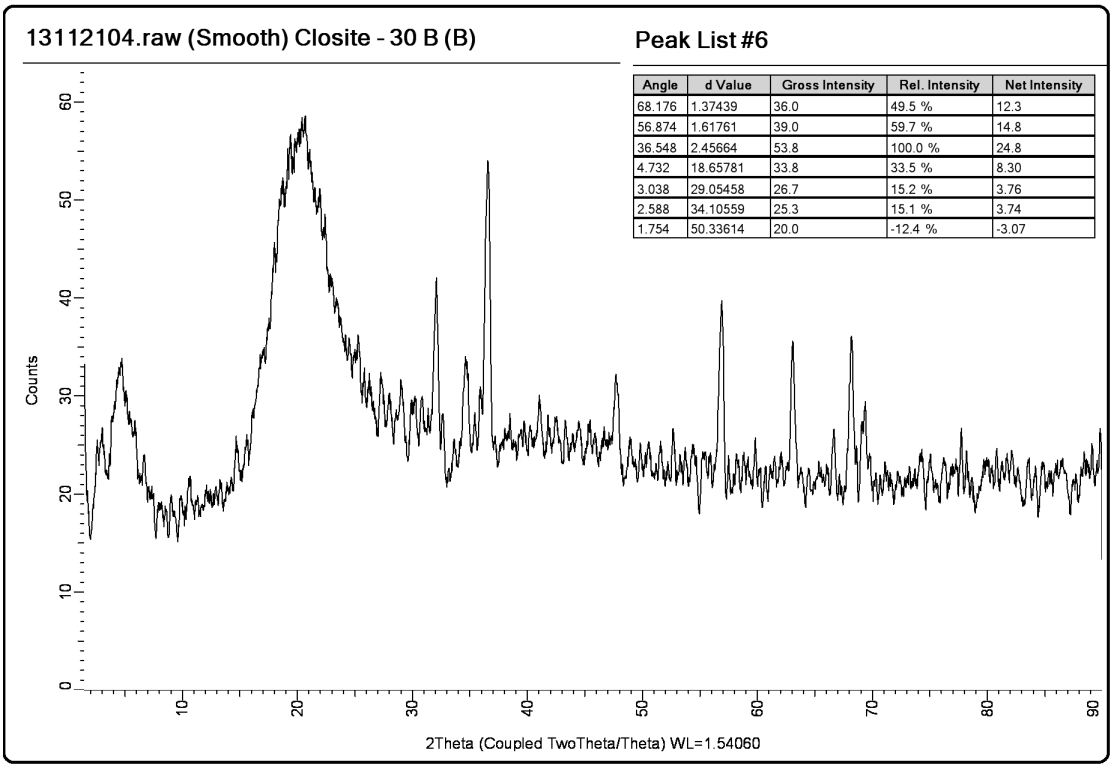

Peak List #6

Angle	d Value	Gross Intensity	Rel. Intensity	Net Intensity
68.176	1.37439	36.0	49.5 %	12.3
56.874	1.61761	39.0	59.7 %	14.8
36.548	2.45664	53.8	100.0 %	24.8
4.732	18.65781	33.8	33.5 %	8.30
3.038	29.05458	26.7	15.2 %	3.76
2.588	34.10559	25.3	15.1 %	3.74
1.754	50.33614	20.0	-12.4 %	-3.07

f) Cloisite 30B-D

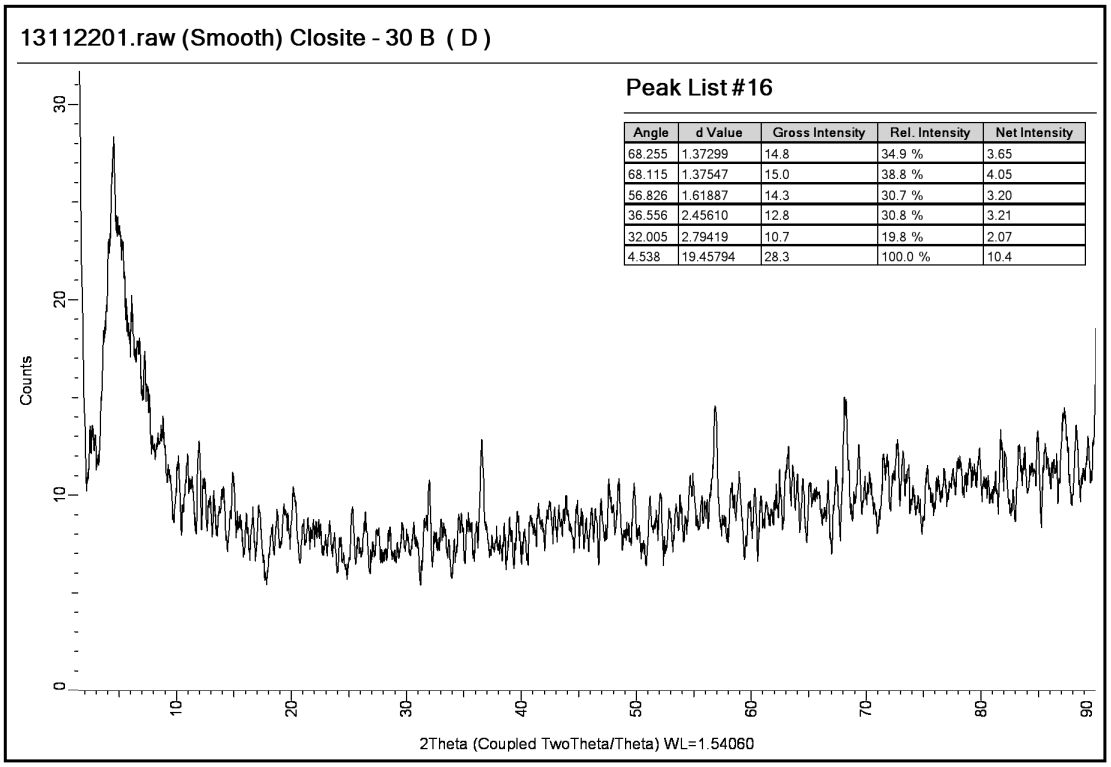

g) Raw CNT powder

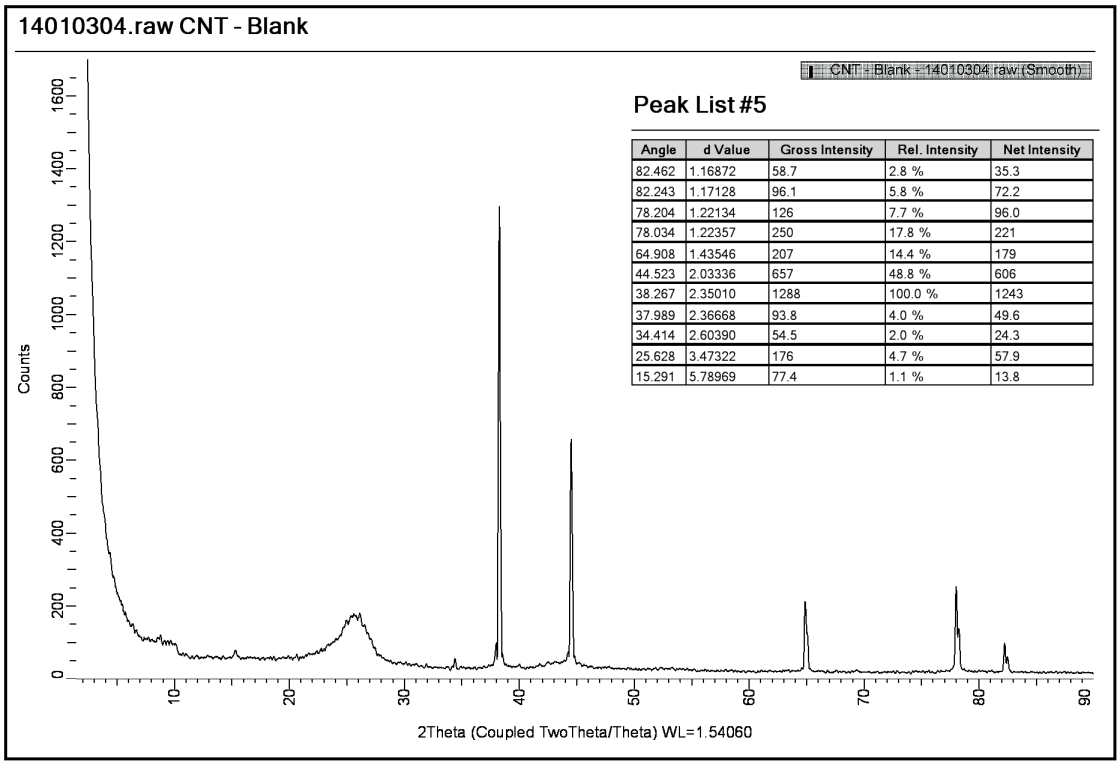

h) CNT-B

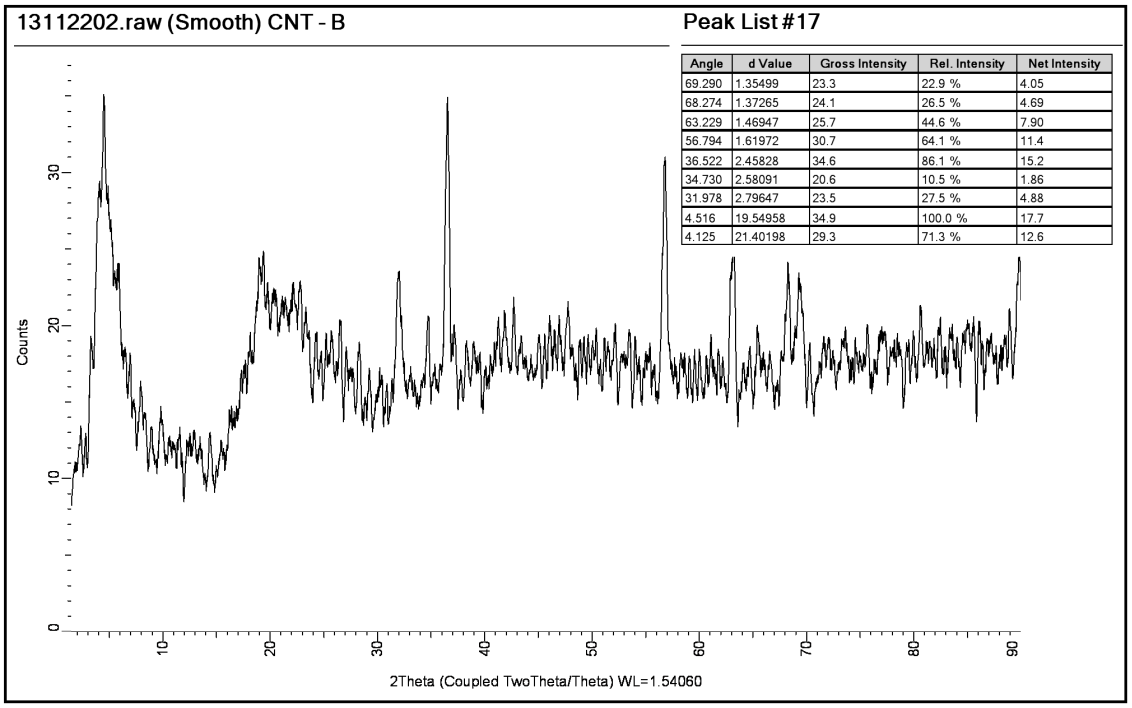
13112202.raw (Smooth) CNT - B
Peak List #17
Angle | d Value | Gross Intensity | Rel. Intensity | Net Intensity
69.290 | 1.35499 | 23.3 | 22.9 % | 4.05
68.274 | 1.37265 | 24.1 | 26.5 % | 4.69
63.229 | 1.46947 | 25.7 | 44.6 % | 7.90
56.794 | 1.61972 | 30.7 | 64.1 % | 11.4
36.522 | 2.45828 | 34.6 | 86.1 % | 15.2
34.730 | 2.58091 | 20.6 | 10.5 % | 1.86
31.978 | 2.79647 | 23.5 | 27.5 % | 4.88
4.516 | 19.54958 | 34.9 | 100.0 % | 17.7
4.125 | 21.40198 | 29.3 | 71.3 % | 12.6
Counts
2Theta (Coupled TwoTheta/Theta) WL=1.54060

i) CNT-D

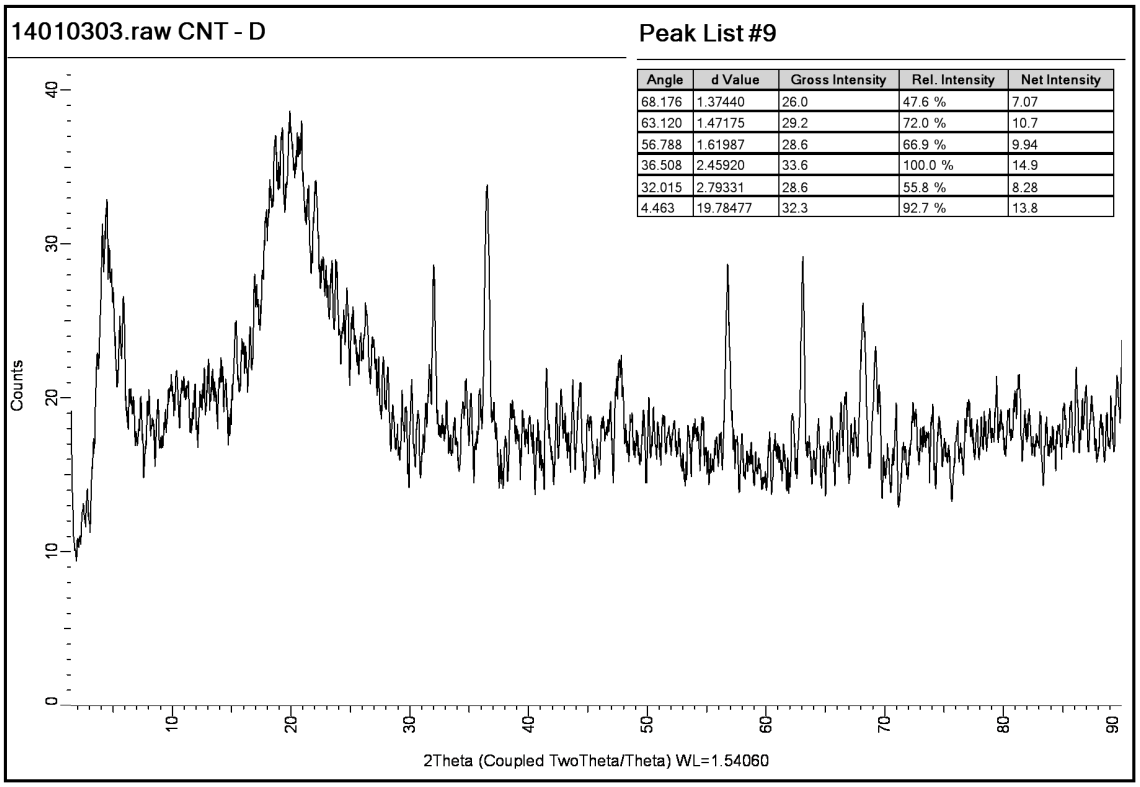
14010303.raw CNT - D
Peak List #9
Angle | d Value | Gross Intensity | Rel. Intensity | Net Intensity
68.176 | 1.37440 | 26.0 | 47.6 % | 7.07
63.120 | 1.47175 | 29.2 | 72.0 % | 10.7
56.788 | 1.61987 | 28.6 | 66.9 % | 9.94
36.508 | 2.45920 | 33.6 | 100.0 % | 14.9
32.015 | 2.79331 | 28.6 | 55.8 % | 8.28
4.463 | 19.78477 | 32.3 | 92.7 % | 13.8
Counts
2Theta (Coupled TwoTheta/Theta) WL=1.54060

j) *In-situ* CNT

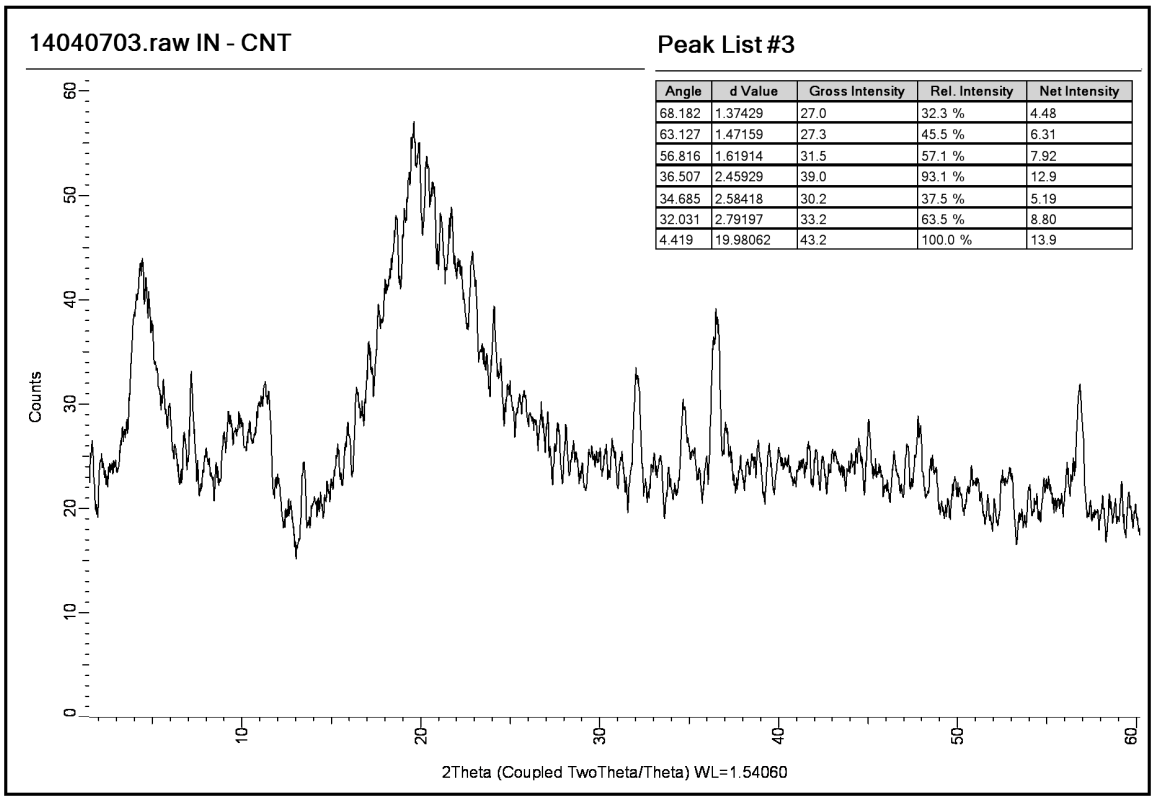
14040703.raw IN - CNT
Peak List #3
Angle | d Value | Gross Intensity | Rel. Intensity | Net Intensity
68.182 | 1.37429 | 27.0 | 32.3 % | 4.48
63.127 | 1.47159 | 27.3 | 45.5 % | 6.31
56.816 | 1.61914 | 31.5 | 57.1 % | 7.92
36.507 | 2.45929 | 39.0 | 93.1 % | 12.9
34.685 | 2.58418 | 30.2 | 37.5 % | 5.19
32.031 | 2.79197 | 33.2 | 63.5 % | 8.80
4.419 | 19.98062 | 43.2 | 100.0 % | 13.9
Counts
0
10
20
30
40
50
60
2Theta (Coupled TwoTheta/Theta) WL=1.54060

Appendix 2

TGA-DSC curves:

Heating range = up to 800°C and heating rate = 10°C per min.

a) BR

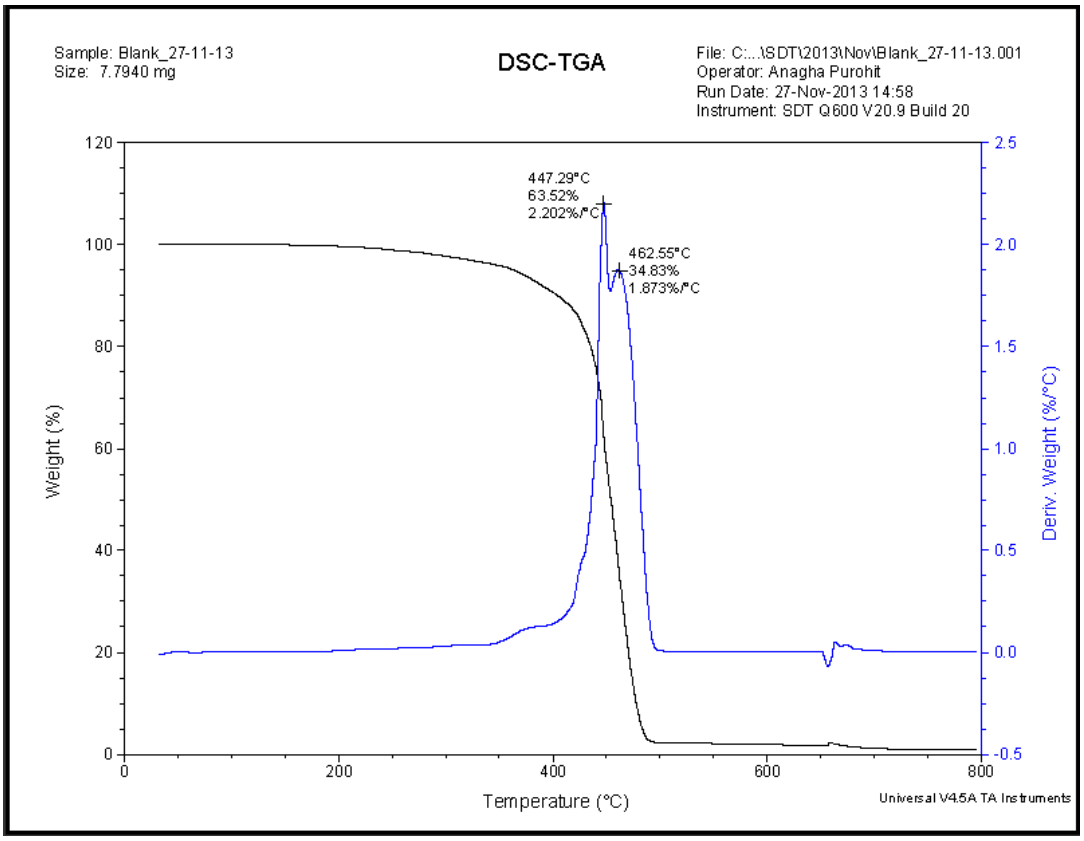

b) BR/Cloisite 20A-B

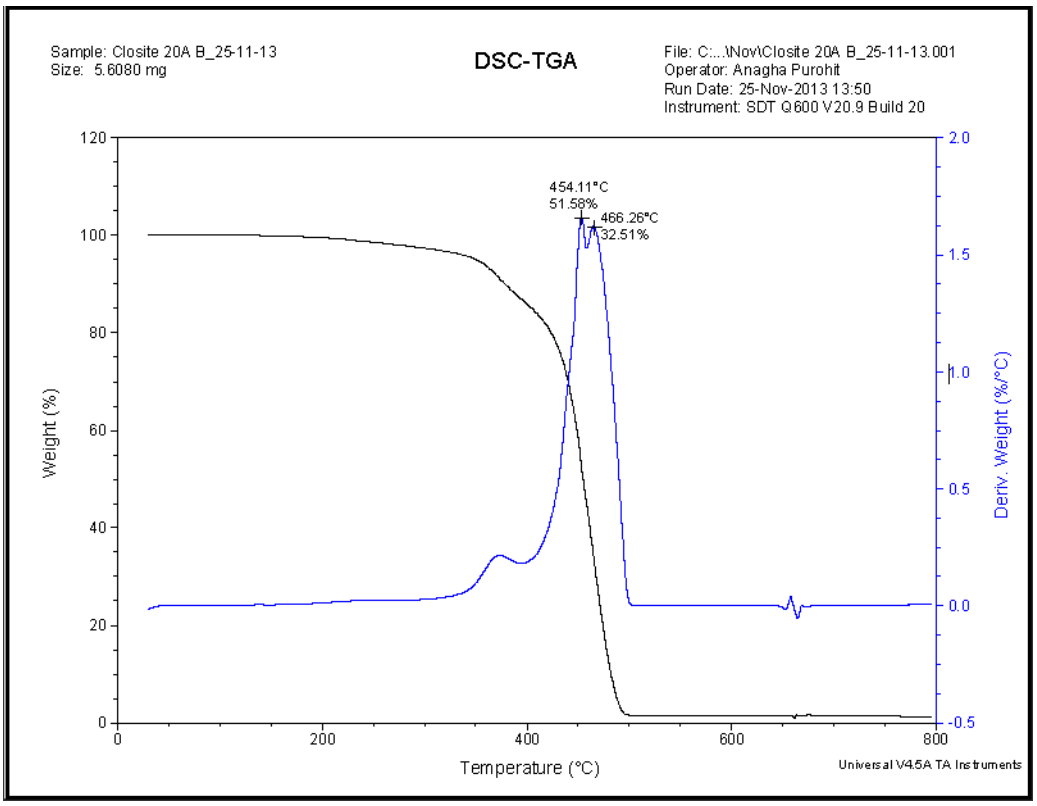

c) BR/Cloisite 30B-B

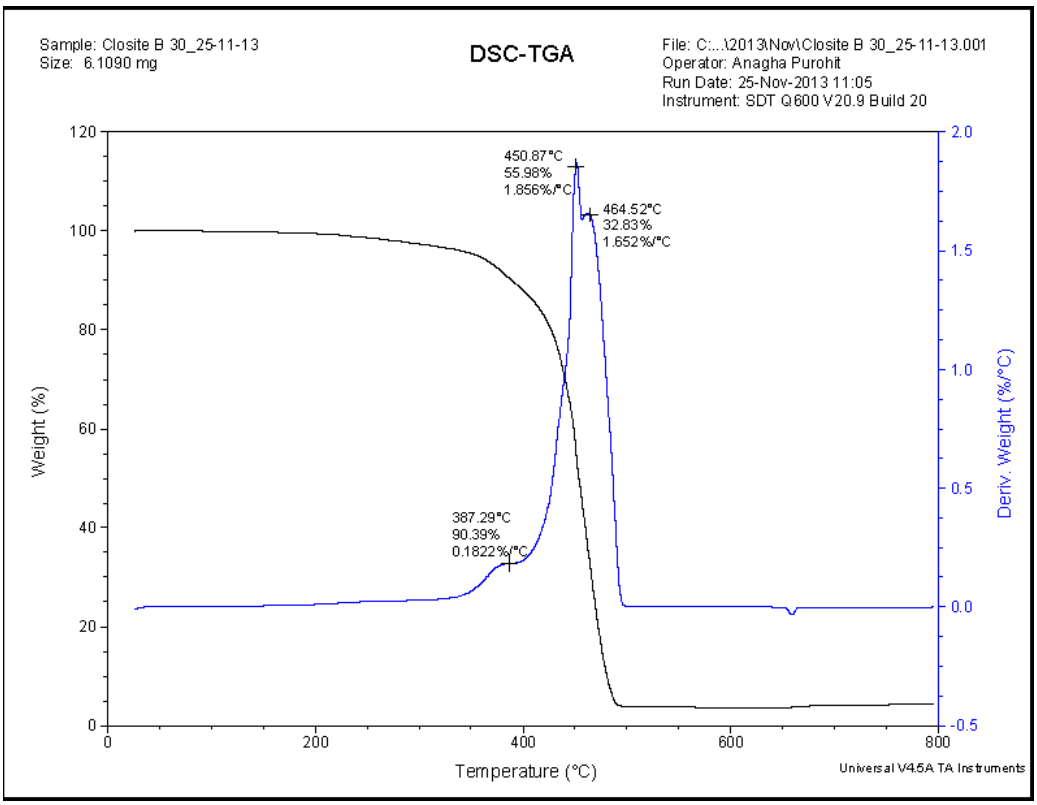

d) BR/CNT B

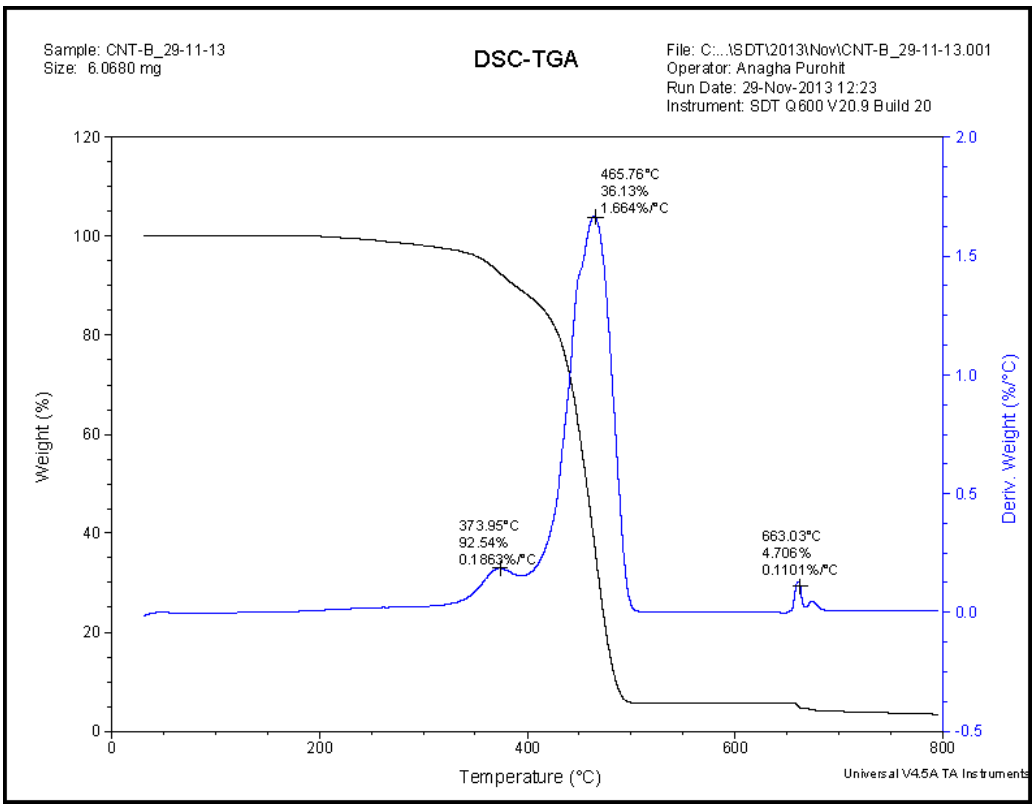

e) BR/CNT D

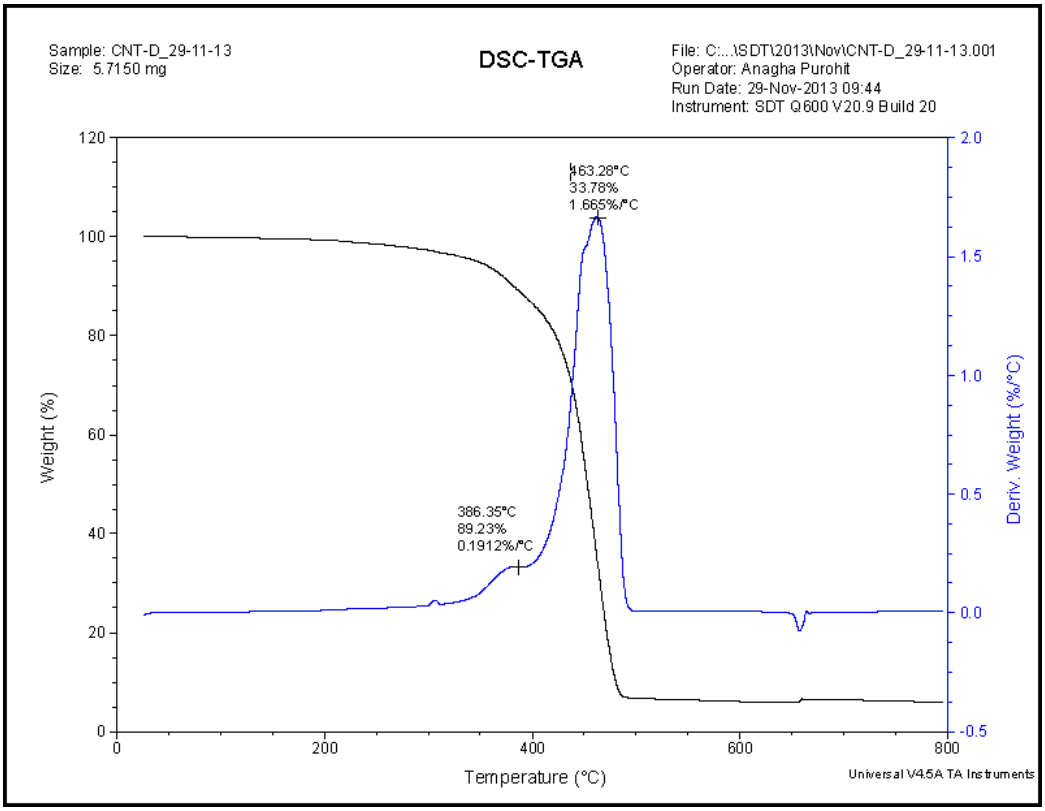

f) BR/Silica-Silane B

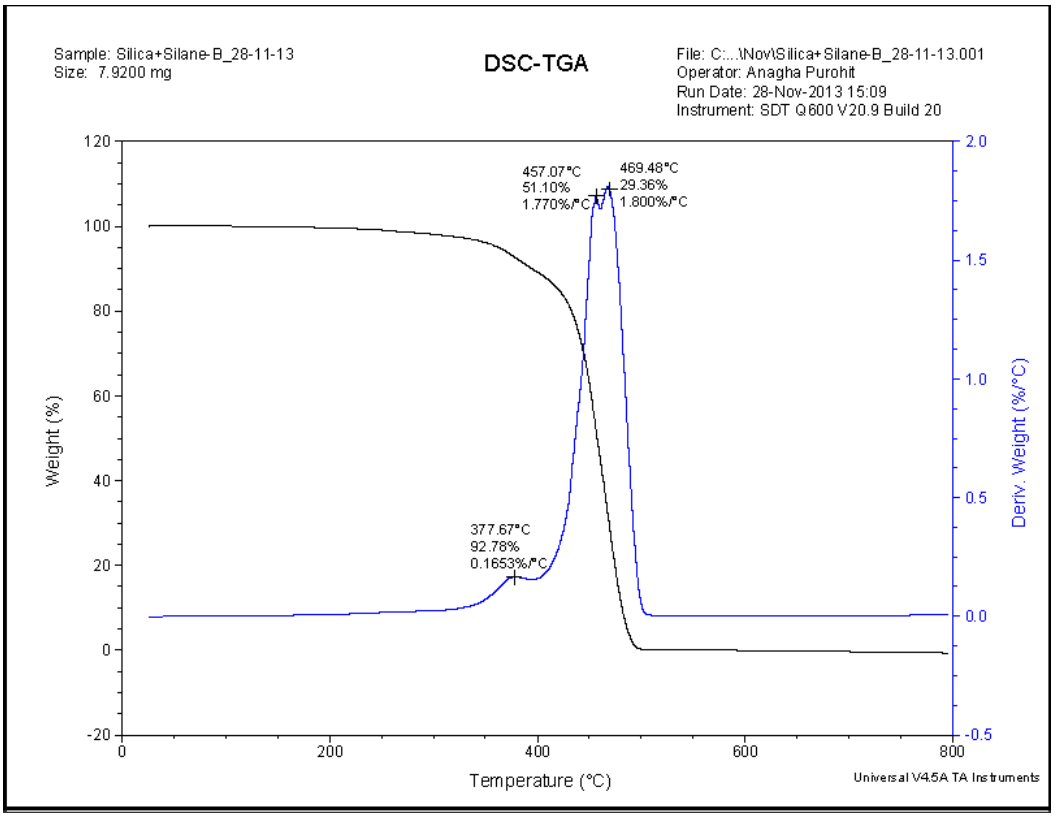

g) BR/In-nanosilica

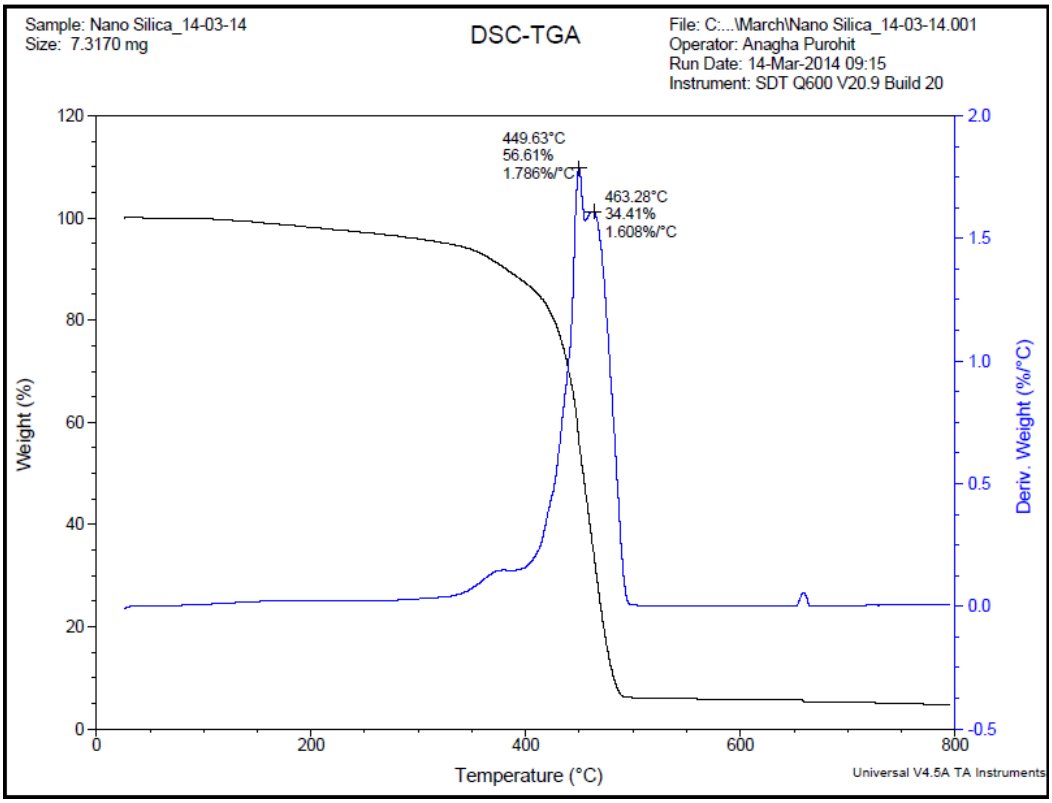

BR/In-CNT

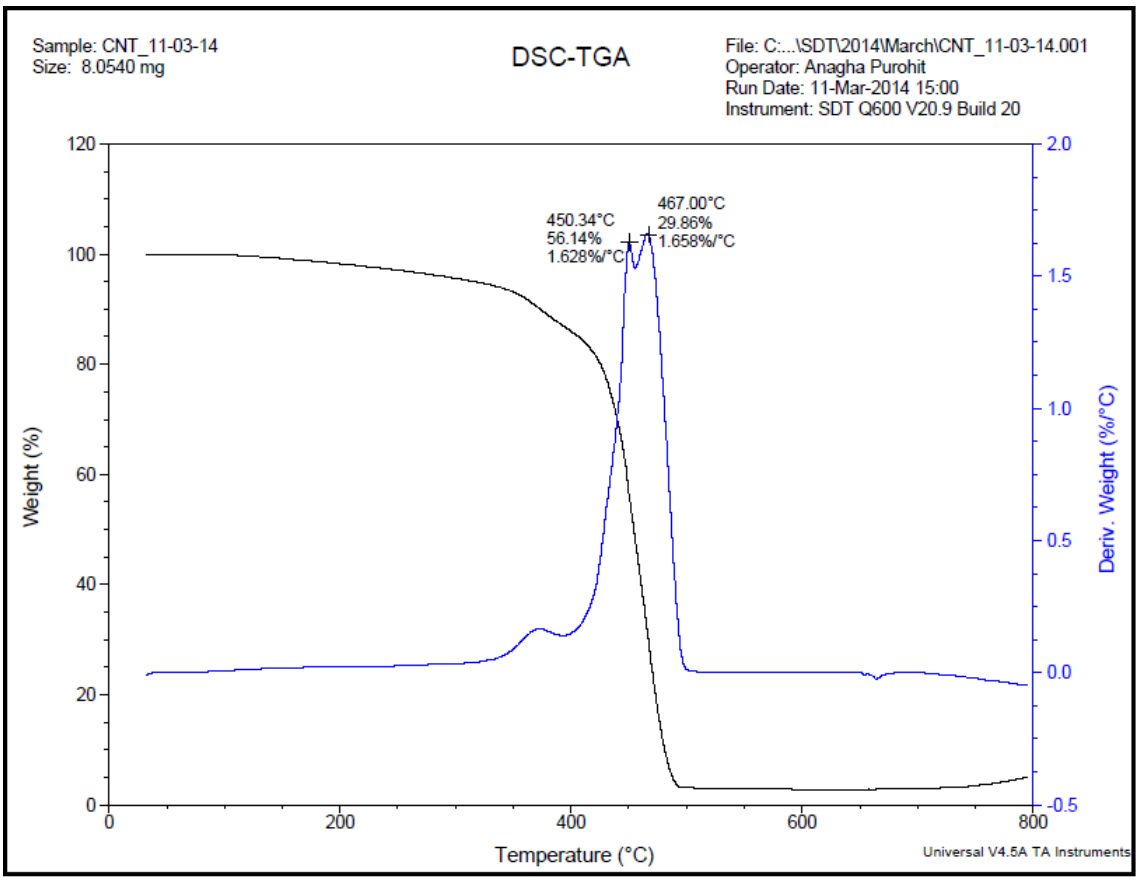
Sample: CNT_11-03-14
Size: 8.0540 mg
DSC-TGA
File: C:...\SDT\2014\March\CNT_11-03-14.001
Operator: Anagha Purohit
Run Date: 11-Mar-2014 15:00
Instrument: SDT Q600 V20.9 Build 20
450.34°C
56.14%
1.628%/°C
467.00°C
29.86%
1.658%/°C
Weight (%)
Deriv. Weight (%/°C)
Temperature (°C)
Universal V4.5A TA Instruments